

# Longitudinal and Transverse Quasi-Elastic Response Functions of Light Nuclei

J. Carlson<sup>a</sup>, J. Jourdan<sup>b</sup>, R. Schiavilla<sup>cd</sup>, I. Sick<sup>b</sup>

<sup>a</sup>Theoretical Division, Los Alamos National Laboratory, Los Alamos, New Mexico, USA

<sup>b</sup>Departement für Physik und Astronomie, Universität Basel, Basel, Switzerland

<sup>c</sup>Jefferson Lab, Newport News, Virginia, USA

<sup>d</sup>Physics Department, Old Dominion University, Norfolk, Virginia, USA

**Abstract.** The  $^3\text{He}$  and  $^4\text{He}$  longitudinal and transverse response functions are determined from an analysis of the world data on quasi-elastic inclusive electron scattering. The corresponding Euclidean response functions are derived and compared to those calculated with Green's function Monte Carlo methods, using realistic interactions and currents. Large contributions associated with two-body currents are found, particularly in the  $^4\text{He}$  transverse response, in agreement with data. The contributions of two-body charge and current operators in the  $^3\text{He}$ ,  $^4\text{He}$ , and  $^6\text{Li}$  response functions are also studied via sum-rule techniques. A semi-quantitative explanation for the observed systematics in the excess of transverse quasi-elastic strength, as function of mass number and momentum transfer, is provided. Finally, a number of model studies with simplified interactions, currents, and wave functions is carried out to elucidate the role played, in the full calculation, by tensor interactions and correlations.

PACS: 21.45.+v, 25.30.Fj

# 1 Introduction

Over the past thirty years or so, much effort has gone into trying to understand quantitatively the roles that short-range and tensor correlations, and two-body components of the nuclear electromagnetic current play in the quasi-elastic response of nuclei at intermediate momentum transfers. Yet, despite the considerable attention that has been devoted to this topic, many open questions remain. Complications arise, in particular, as a consequence of the need of (and technical difficulties associated with) providing an accurate description of the initial bound- and the final scattering-state wave functions, based on realistic Hamiltonians.

In part, the slow progress is also due to the confusing experimental picture, particularly for medium- and heavy-weight nuclei, that for some time obfuscated the interpretation of the data. Early data [1] had shown that, in comparison to an impulse-approximation (IA) calculation using a simple (Fermi gas) model, the inclusive cross section showed an excess of transverse strength, mainly in the region of the “dip” between the quasi-elastic and the  $\Delta$  peaks. This excess was attributed to two-body currents and  $\pi$ -production, but not quantitatively understood.

The longitudinal and transverse response functions, obtained during the eighties from a Rosenbluth separation of experimental cross sections, seemed to indicate that, in addition, there was a gross (up to 40%) lack of *longitudinal* strength in the main quasi-elastic peak, and a correspondingly too low Coulomb sum rule [2, 3]. While this state of affairs is yet to be resolved satisfactorily, particularly for very heavy nuclei like lead, where Coulomb corrections are difficult [4, 5, 6, 7] there are nevertheless clear indications for  $A \leq 56$  from the work of Jourdan [8], who carefully analyzed the *world* data on quasi-elastic scattering including all the known corrections, that there is no missing strength in the longitudinal response of medium-A nuclei (for very heavy nuclei, there are still controversial issues on the Coulomb corrections, see Refs. [9, 10, 11]). This apparent lack of longitudinal strength has absorbed much of the theoretical effort of the past two decades.

On the other hand, the excess of transverse strength — presumably due to two-body currents — observed in the quasi-elastic region appears to be a genuine problem. In this respect, the experimental situation has been put in sharp focus by the work on super-scaling by Donnelly and Sick [12] which allowed to systematically compare the longitudinal and transverse response functions. This work showed in the most clear way that the transverse strength for nuclei with mass number  $A=12, \dots, 56$  exceeds the longitudinal one already in the main quasi-elastic peak by 20-40%, in addition to the excess of strength occurring in the “dip” between the quasi-elastic and  $\Delta$ -peaks. This excess of strength in the region of the quasi-elastic peak is the main subject of this paper. The region of the dip, which has attracted the attention in the past, will be largely ignored as the understanding of this region is clouded by issues relating to pion production and the  $\Delta$ -tail.

Theoretical calculations of two-body contributions in the region of the quasi-elastic peak have been performed by many groups [13]– [26] using different approaches. Some of

these calculations find appreciable contributions, 20–40% of the transverse response, due to the dominant two-body terms (pion contact and in-flight, and  $\Delta$ -excitation diagrams), other calculations find small, <10%, effects. It is not always clear why calculations with similar starting assumptions give very different results.

In general, calculations based on an independent-particle initial state (shell model, Fermi gas model, possibly with RPA correlations added) give very small two-body contributions in the quasi-elastic peak [13]–[20], [23, 26]: the pion and  $\Delta$  terms tend to cancel to produce a small overall effect. The origin of bigger (20–50%) contributions to the transverse response as obtained in Refs. [22, 25] is not entirely understood: the different treatment of the  $\Delta$  in matter in Ref. [22] may be partly responsible [27].

The model study of Leidemann and Orlandini [17], in which the nuclear response was expressed in terms of the response of deuteron-like pairs of nuclear density, first pointed out that it is important to account in the initial state for the *tensor* correlations between  $np$  pairs. Only when these (rather short-range) tensor correlations were included would the two-body terms give appreciable contributions to the quasi-elastic response. This insight was quantitatively confirmed by Fabrocini [24], who calculated the transverse response of infinite nuclear matter using correlated basis function theory including one-particle-one-hole intermediate states. This calculation is based on a realistic nucleon-nucleon (N-N) interaction and two-body terms derived consistently from the N-N interaction, and accounts for the interactions in both the initial and final states. It also found that substantial two-body contributions in the quasi-elastic peak are obtained only if the tensor correlations, predominantly induced by pion exchange, are retained.

The calculation of Carlson and Schiavilla [21] was performed for  $^4\text{He}$  using Green’s function Monte Carlo (GFMC) techniques, a realistic (Argonne  $v'_8$ ) N-N interaction and again consistently constructed two-body terms. The inelastic response could be accurately calculated in terms of the Euclidean response (an integral over the response function, see below). These “exact” calculations found that the charge-exchange character of the N-N interaction leads to shifts of both the longitudinal and transverse strength to higher excitation energies, thus producing a quenching of the response in the region of the quasi-elastic peak. This mechanism, however, is more than offset in the transverse channel by two-body currents, in particular those associated with pion exchange (required by gauge invariance), and hence the response is enhanced over the entire quasi-elastic spectrum. This enhancement was found to be substantial, and in agreement with that observed experimentally. The study of Ref. [21], while providing a qualitative understanding of the  $^4\text{He}$  quasi-elastic response, did not identify quantitatively, however, those aspects of the calculation responsible for the successful prediction.

In the present paper we study the longitudinal and transverse response functions of light nuclei,  $^3\text{He}$  and  $^4\text{He}$ , using GFMC theory. Accurate data for these responses in the region of the quasi-elastic peak are determined via an analysis of the world data. A simultaneous study of  $^3\text{He}$  and  $^4\text{He}$  is particularly interesting as the predicted two-body contributions in the transverse channel increase very rapidly between  $A=3$  and

$A=4$ , a feature which can give us a further handle for the understanding of two-body effects. The study of  $^4\text{He}$ , including the higher momentum transfers now available, is especially promising, since the available data [8] seem to indicate that the relative excess of transverse strength in the quasi-elastic peak is largest for this nucleus. In order to include heavier nuclei and hence examine the evolution with mass number of this excess transverse strength, we also study via sum-rules the two-body contributions for p-shell nuclei, for which variational Monte Carlo (VMC) wave functions are available.

The layout of this paper is as follows. In Sec. 2 we discuss the determination of the longitudinal and transverse response functions starting from the world data on inclusive electron scattering, while in Sec. 3 we perform a scaling analysis in order to investigate the global properties of the experimental response. In Sec. 4 we describe the theory of the Euclidean responses which link the nuclear ground-state properties to integral properties of the electromagnetic response as measured in  $(e,e')$ , and in Sec 5 present the model adopted for the nuclear electromagnetic current. Before comparing theory with experiment (Sec. 7), we carry out in Sec. 6 a model study of the relation between the inclusive cross section and the Euclidean response in order to better understand the characteristics of the latter. An extension of the study to heavier nuclei via sum rules is given in Sec. 8, in which the dependence of the excess transverse strength upon mass number is examined. In Sec. 9 we further analyze the calculated results by introducing various simplifications, so as to identify the most important aspects of the calculations. Finally, in Sec. 10 we summarize our conclusions.

## 2 Experimental response functions

In order to determine the longitudinal ( $L$ ) and transverse ( $T$ ) responses, we have analyzed the  $(e,e')$  world data on  $^3\text{He}$  and  $^4\text{He}$ . A determination of the response functions in inclusive quasi-elastic scattering from the world cross section data has many advantages over the traditional approach of using data from a single experiment only. Particularly for medium- $A$  nuclei the limitations of the traditional approach was partly responsible for the misleading conclusions mentioned in the introduction and discussed in [8].

For the extraction of the response functions, the difference of cross sections at high-energy/forward-angle and at low-energy/backward-angle is used. Kinematics dependent systematic errors do not cancel in this difference even for measurements performed at a single facility, except perhaps for the errors in the overall normalization of the cross sections. The dominant systematic errors, *i.e.* uncertainties in the spectrometer acceptance, detector efficiencies, background contributions, re-scattering, and radiative corrections are strongly dependent on the specific kinematics.

To improve the determination of the response functions the difference of the  $L$ - and  $T$ -contributions to the cross sections has to be maximized by including data over the largest possible angular range. This can only be achieved by including all available world

cross section data. For  ${}^3\text{He}$  and  ${}^4\text{He}$  the use of the world data not only expands the range of available data in scattering angle but also increases the range of momentum transfer  $q$  where a separation can be done, thus leading to new information on the response functions.

At low  $q$  the extensive sets of data for  ${}^3\text{He}$  [28, 29] and for  ${}^4\text{He}$  [30, 31] with good angular coverage have been used in the present analysis. For  ${}^3\text{He}$  at high  $q$  the data by Marchand *et al.* [28] and by Dow *et al.* [29], which both cover the angular region from  $90^\circ$  to  $144^\circ$ , are combined with complementary cross sections by Day *et al.* [32] which provide high-energy/forward-angle data with energies up to 7.2 GeV at scattering angles of  $8^\circ$ . Similarly for  ${}^4\text{He}$  the data by Zghiche *et al.* [30], which cover the angular region from  $75^\circ$  to  $145^\circ$ , and by Dytman *et al.* [31] which contribute data at  $60^\circ$ , are complemented with the forward angle cross sections by Rock *et al.* [33], Day *et al.* [34], Sealock *et al.* [35], and Meziani *et al.* [36] covering the angular range from  $8^\circ$  to  $37^\circ$ .

In contrast to the analysis performed for medium- $A$  nuclei [8], Coulomb distortions play a negligible role for  ${}^3\text{He}$  and  ${}^4\text{He}$  and no corrections need to be applied. The following expression, valid in the plane wave Born approximation (PWBA), is used for the Rosenbluth or  $L/T$ -separation:

$$\Sigma(q, \omega, \epsilon) = \frac{d^2\sigma}{d\Omega d\omega} \frac{1}{\sigma_{Mott}} \epsilon \left(\frac{q}{Q}\right)^4 = \epsilon R_L(q, \omega) + \frac{1}{2} \left(\frac{q}{Q}\right)^2 R_T(q, \omega) , \quad (1)$$

where the longitudinal virtual photon polarization  $\epsilon$  is defined as

$$\epsilon = \left(1 + \frac{2q^2}{Q^2} \tan^2 \frac{\vartheta}{2}\right)^{-1} , \quad (2)$$

and varies between 0 to 1 as the electron scattering angle  $\vartheta$  ranges from  $180$  to  $0$  degrees. Here,  $d^2\sigma/d\Omega d\omega$  are the experimental cross sections,  $\omega$ ,  $q$  and  $Q$  are the energy transfer, 3- and 4-momentum transfers, respectively, and  $\sigma_{Mott}$  is the Mott cross section. The structure of Eq. (1) shows that measurements of the cross section at fixed  $\omega$  and  $q$  but different  $\epsilon$  allow for a separation of the two response functions  $R_L(q, \omega)$  and  $R_T(q, \omega)$ .

In practice, the experimental spectra of the various experiments were measured for a given incident energy and scattering angle as a function of the energy loss of the scattered electron, varied by changing the magnetic field of the spectrometer. To determine the cross section at given values of  $q$  and  $\omega$ , the data have to be interpolated. This traditionally was done by dividing out  $\sigma_{Mott}$  from the measured cross sections and interpolating the responses along  $\omega/E$ .

In an analysis of the world data, where the various experiments were not planned for an ideal coverage of the  $q$ - $\omega$ -plane, the usual scheme is unreliable due to occasionally large spacings between various spectra. Thus, in the present analysis an improved scheme is employed by first dividing out an appropriate sum of elementary electron-nucleon cross sections, *i.e.*  $\sigma_{ep}$  for the proton and  $\sigma_{en}$  for the neutron, and removing kinematical dependencies. Essentially what is calculated from the data is the scaling function  $F(y, q)$

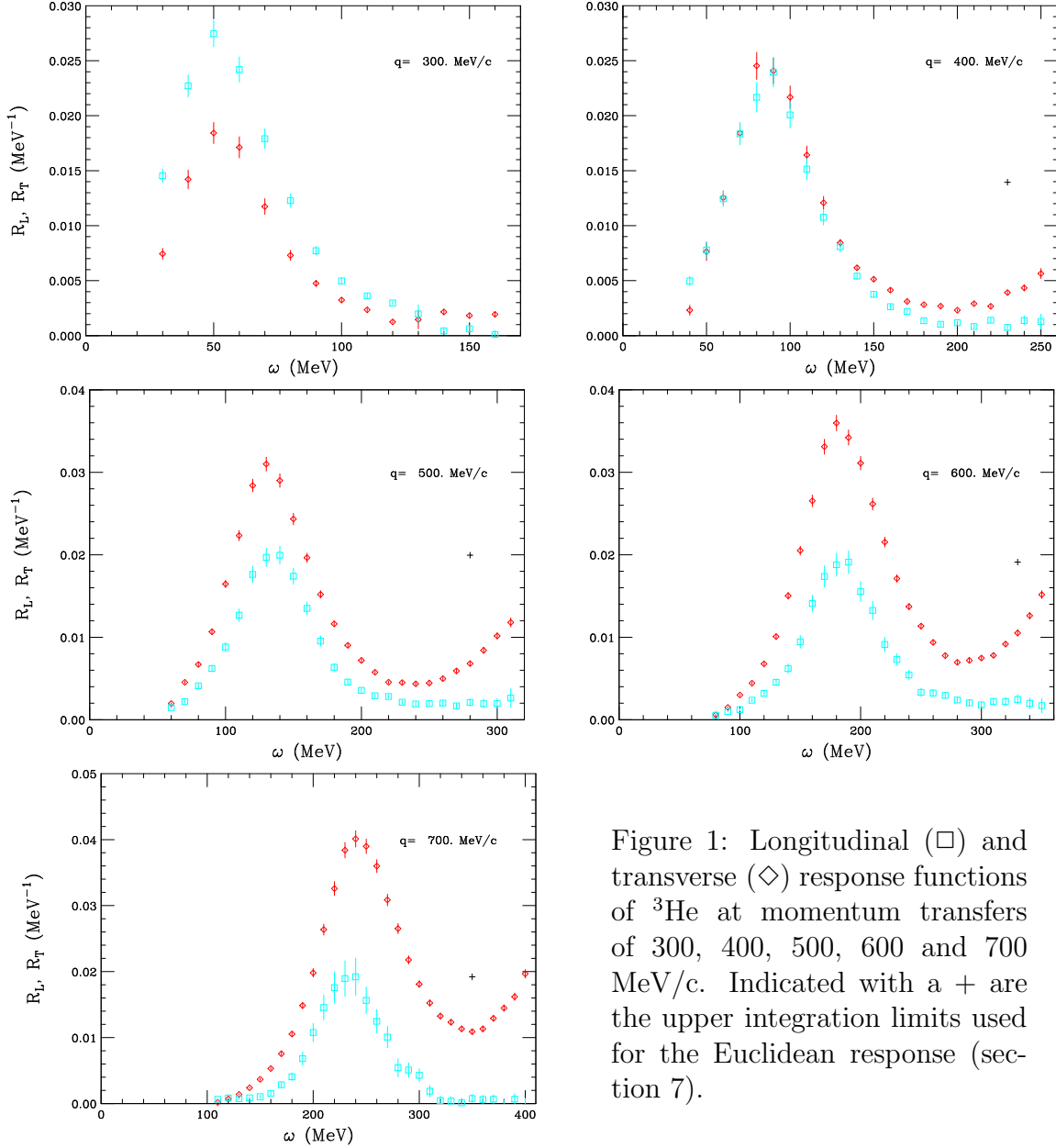


Figure 1: Longitudinal ( $\square$ ) and transverse ( $\diamond$ ) response functions of  ${}^3\text{He}$  at momentum transfers of 300, 400, 500, 600 and 700 MeV/c. Indicated with a + are the upper integration limits used for the Euclidean response (section 7).

defined by

$$F(y, q) = \frac{d^2\sigma}{d\omega d\Omega} \frac{1}{Z\sigma_{ep}(q) + N\sigma_{en}(q)} \frac{d\omega}{dy}. \quad (3)$$

The scaling variable  $y$  is fixed by energy and momentum conservation via

$$y = -q + \sqrt{\omega^2 + 2\omega m}, \quad (4)$$

neglecting small contributions from the binding energy, the perpendicular component of the nucleon momentum, and the recoil energy of the residual nucleus. In the next phase of the analysis, the extracted  $F(y, q)$  are then used to determine  $F(y, q_0)$  at the desired value  $q_0$  by interpolating  $F(y, q)$  along lines of constant  $y$ .

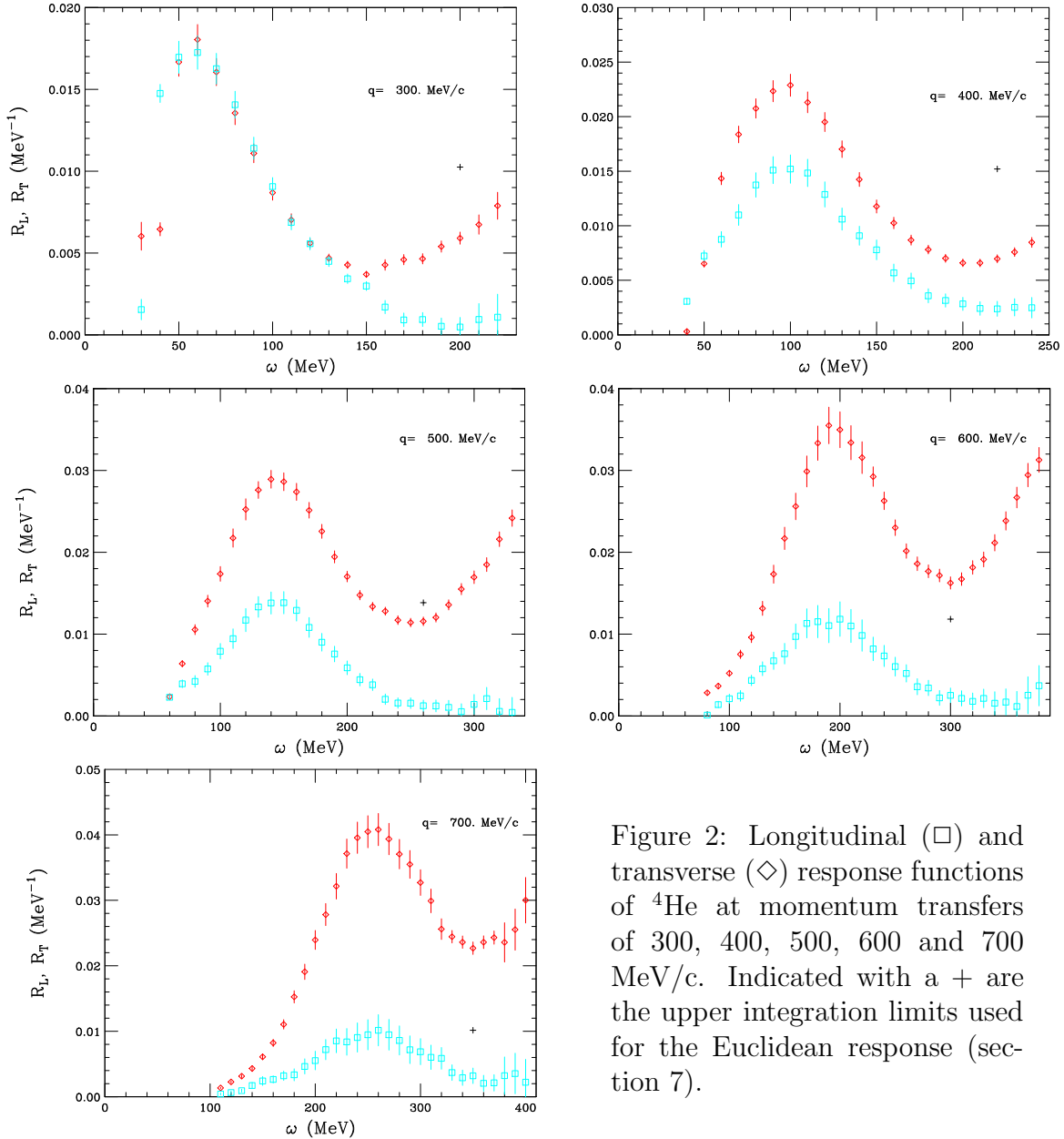


Figure 2: Longitudinal ( $\square$ ) and transverse ( $\diamond$ ) response functions of  ${}^4\text{He}$  at momentum transfers of 300, 400, 500, 600 and 700 MeV/c. Indicated with a + are the upper integration limits used for the Euclidean response (section 7).

For  $y < 0$ ,  $F(y, q)$  is known to be nearly independent of  $q$  over a large range. This makes the present interpolation as reliable as the conventional interpolation scheme even if the data are separated by large values of  $q$ . For  $y > 0$ , the dependence of  $F(y, q)$  on  $q$  is relatively more severe, since inelastic processes contribute to the cross section. Thus, the  $q$ -value of the  $L/T$ -separation has been chosen to minimize the correction due to the interpolation at large  $\omega$ .

The interpolation procedure and the separation has been tested with the data of the Saclay experiments [30, 28] alone. Provided the same interpolation scheme is used, the published values of  $R_L(q, \omega)$  and  $R_T(q, \omega)$  are reproduced exactly. The improved interpolation scheme, using  $y$ -scaling, gives results which also are identical within the

statistical errors.

With the interpolated cross section data, the response functions are extracted for  $q=300\text{--}700$  MeV/c in steps of 100 MeV/c for both nuclei. The combined world data cover almost the full  $\epsilon$ -range, with typical values ranging from 0.05 to 0.95 for most  $q$ -sets. At high  $q$  this has to be compared with the results of the low energy data alone which only cover the region from 0.05 to 0.55. In addition, with a global analysis it is possible to determine for the first time the response functions at  $q=700$  MeV/c.

If the interpolated responses of data are plotted as a function of  $\epsilon$ , a linear dependence is expected. In contrast to the analysis of medium- $A$  nuclei, in which important deviations were observed for high  $q$  and  $\omega$ , no significant deviations were observed in the present analysis once the quoted systematic errors of the individual data sets are included.

The longitudinal and transverse response functions resulting from this analysis of the *world* data are shown in Figs. 1 and 2.

### 3 Scaling analysis

In order to show the excess strength of  $R_T(q, \omega)$ , in this section we study the scaling properties of the present response functions. Barbaro *et al.* [37] have discussed the close connection between the Coulomb sum rule and the notion of  $y$ -scaling. More recently the notion of  $\psi'$ -scaling was introduced by Alberico [38] while studying the properties of the relativistic Fermi gas model. The application of this notion to finite nuclear systems, requiring the inclusion of binding effects, has been discussed by Cenni *et al.* [39]. Guided by these results, Sick and Donnelly have applied  $\psi'$ -scaling to a large body of inclusive scattering data [12]. Scaling in  $\psi'$  has the merit to allow the study of the scaling properties for a combined set of *different* nuclei. The only relevant scale parameter in the quasi-free scattering regime is the Fermi momentum of the nucleus which is taken into account in the definition of the dimensionless scaling variable  $\psi'$  (approximately given by  $y/k_F$ ), and the scaling function  $f(\psi')$ .

As discussed in [12],  $\psi'$ -scaling can also be studied for separated response functions. The dimensionless scaling functions  $f_{L,T}$  are defined in [12] as

$$f_{L,T} \equiv k_F \frac{R_{L,T}}{G_{L,T}} , \quad (5)$$

with the factors  $G_{L,T}$  given in [12]. For the relativistic Fermi gas model and in IA, the universal relation

$$f_L = f_T = f \quad (6)$$

is predicted. Neglecting powers higher than two in  $\eta_F = k_F/m$ , a relation between  $f_L$  and the Coulomb sum rule is obtained as

$$\int d\psi f^{RFG}(\psi) = 1 + \frac{1}{20}\eta_F^2 + \dots . \quad (7)$$



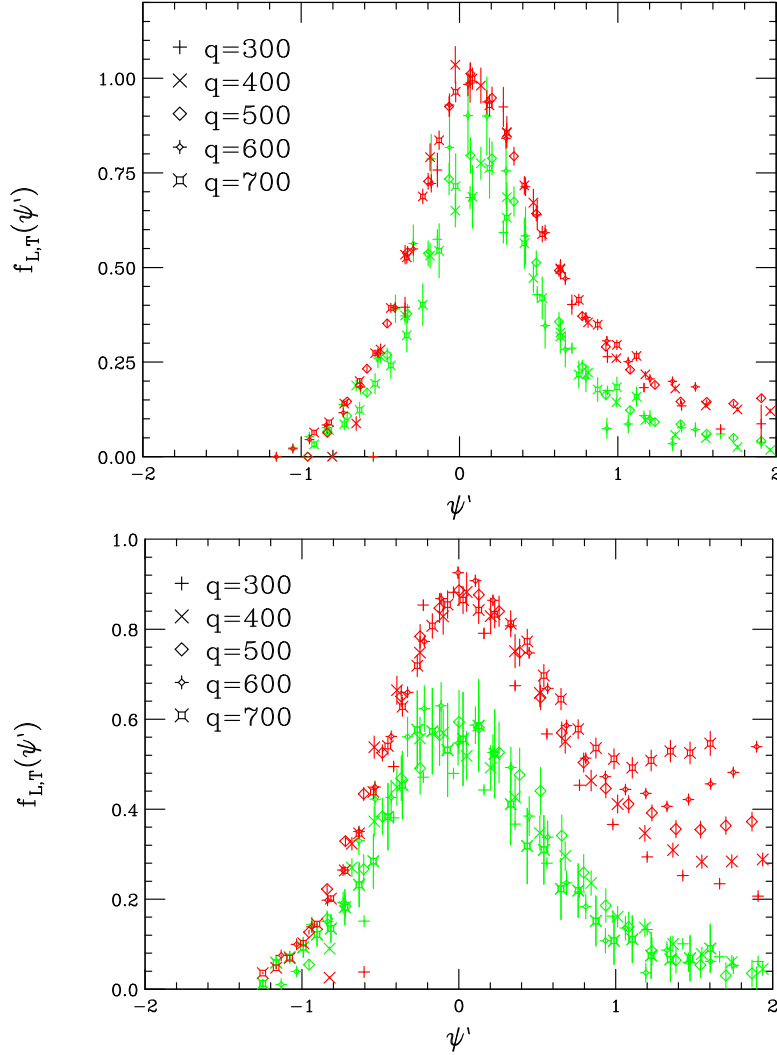


Figure 3: The scaling functions  $f_L$  and  $f_T$  are shown for all  $q$  values on the top for  ${}^3\text{He}$  and on the bottom for  ${}^4\text{He}$ . The upper bands of points correspond to  $f_T$ , the lower bands to  $f_L$ .

In Fig. 3 we compare the scaling functions  $f_L(\psi')$  and  $f_T(\psi')$  obtained for all response functions extracted from the global analysis of the  ${}^3\text{He}$  and  ${}^4\text{He}$  data. Within the error bars of the separated data, the longitudinal response functions scale to a universal curve over the entire quasi-elastic peak. Scaling of  $R_L(q, \omega)$  is expected and provides a consistency check for the Coulomb sum rule. The results for  $R_T(q, \omega)$  confirm that the basic problem in quasi-elastic electron-nucleus scattering is the *excess strength in the transverse response*. This excess is much larger for  ${}^4\text{He}$  than for  ${}^3\text{He}$ . Scaling is also observed for  $R_T(q, \omega)$  at negative values of  $\psi'$ , thus suggesting that processes other than quasi-free knock out can also lead to scaling.

The excess of transverse strength is particularly large for  ${}^4\text{He}$ . It exceeds the longitudinal strength at all momentum transfers, and does not seem to be limited to the “dip” region, but affects the whole quasi-elastic peak region, extending below the  $\pi$ -production threshold. The transverse strength in the dip, which increases with increasing  $q$ , is related to the growing overlap between the high-energy side of the quasi-elastic peak and the tail of the  $\Delta$ -peak.

In order to study the  $A$ -dependence of this excess, we can look at the longitudinal and transverse responses integrated over  $\psi'$  — those for  ${}^{12}\text{C}$ ,  ${}^{40}\text{Ca}$ , and  ${}^{56}\text{Fe}$  have been determined in Ref. [12]. We have integrated these responses over the region of  $\psi'$  that essentially covers the quasi-elastic peak ( $|\psi'| < 1.2$ ). When limiting the integration range to  $|\psi'| < 0.5$  much of the contribution from the tail of the  $\Delta$  is eliminated, at least for the light nuclei. The ratio of transverse to longitudinal integrated strength is shown in Fig. 4.

Figure 4 makes it clear that: i) the excess of transverse strength rises very rapidly between  ${}^3\text{He}$  and  ${}^4\text{He}$ , and is indeed largest for  ${}^4\text{He}$ ; ii) it is already large at the lowest  $q$ , the increase at the larger  $q$  for the heavier nuclei is mainly due to the fact that the tail of the  $\Delta$  peak contributes appreciably despite the restricted range of integration in  $\psi'$ .

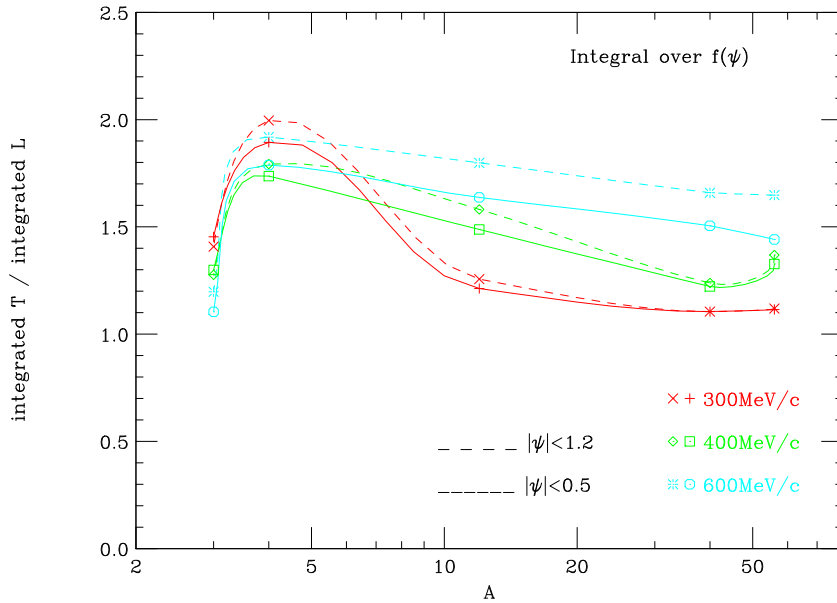


Figure 4: Ratio of transverse to longitudinal integrated strength for  ${}^3\text{He}$ ,  ${}^4\text{He}$ ,  ${}^{12}\text{C}$ ,  ${}^{40}\text{Ca}$ , and  ${}^{56}\text{Fe}$ : 300 MeV/c: x and +, 400 MeV/c:  $\diamond$  and  $\square$ , 600 MeV/c: \* and o. Points at the same  $q$  are joined by lines. The integrations are over the indicated ranges of  $\psi'$ .

## 4 Calculations of Euclidean response

Since we are primarily concerned with the overall strength of the longitudinal and transverse response, we consider the Euclidean response functions, defined as [21, 40]

$$\tilde{E}_{T,L}(q, \tau) = \int_{\omega_{\text{th}}}^{\infty} \exp[-(\omega - E_0)\tau] R_{T,L}(q, \omega) , \quad (8)$$

where the  $R_{T,L}(q, \omega)$  are the standard responses,  $E_0$  is the ground-state energy of the nucleus, and  $\omega_{\text{th}}$  is the threshold for the response of the system excluding the elastic contribution. The longitudinal and transverse Euclidean response functions represent weighted sums of the corresponding  $R_L(q, \omega)$  and  $R_T(q, \omega)$ : at  $\tau=0$  they correspond to the Coulomb and transverse sum rules, respectively, while their derivatives with respect to  $\tau$  evaluated at  $\tau=0$  correspond to the energy-weighted sum rules. Larger values of  $\tau$  correspond to integrals over progressively lower-energy regions of the response.

In a non-relativistic picture, the  $E_{T,L}$  can be simply obtained from:

$$\tilde{E}_L(q, \tau) = \langle 0 | \rho^\dagger(\mathbf{q}) \exp[-(H - E_0)\tau] \rho(\mathbf{q}) | 0 \rangle - \exp\left(-\frac{q^2\tau}{2Am}\right) |\langle 0(\mathbf{q}) | \rho(\mathbf{q}) | 0 \rangle|^2, \quad (9)$$

$$\tilde{E}_T(q, \tau) = \langle 0 | \mathbf{j}_T^\dagger(\mathbf{q}) \exp[-(H - E_0)\tau] \mathbf{j}_T(\mathbf{q}) | 0 \rangle - \exp\left(-\frac{q^2\tau}{2Am}\right) |\langle 0(\mathbf{q}) | \mathbf{j}_T(\mathbf{q}) | 0 \rangle|^2 \quad (10)$$

where the elastic contributions have been explicitly subtracted,  $|0(\mathbf{q})\rangle$  represents the ground state recoiling with momentum  $\mathbf{q}$ , and sums over spin projections are understood.

In this paper we present results for the scaled Euclidean responses

$$E_{L,T}(q, \tau) = \frac{\exp[q^2\tau/(2m)]}{[G_{E,p}(\tilde{Q}^2)]^2} \tilde{E}_{L,T}(q, \tau) , \quad (11)$$

where  $\tilde{Q}^2$  is the squared four-momentum transfer evaluated at the quasi-elastic peak. This removes the trivial energy dependence obtained from scattering off an isolated (non-relativistic) nucleon, and the  $q$  dependence associated with the nucleon form factors. The longitudinal response  $E_L(q, \tau)$  is unity for an isolated proton, and the transverse response  $E_T(q, \tau)$  is simply the square of its magnetic moment.

The chief advantage of formulating the Euclidean response is that it can be calculated exactly using Green's function or path integral Monte Carlo techniques, including both final state interactions and two-nucleon currents. While the present calculations consider only  $A$  up to 4, they can be very simply extended to mass up to  $A=10$  in direct analogy with ground-state calculations [41]. In the future it may be possible to use the Auxiliary-Field Diffusion Monte Carlo technique developed by Schmidt and Fantoni [42] to calculate the response for much heavier systems.

Other techniques have also been used to calculate the response in few-nucleon systems, including Faddeev methods [43, 44] and Lorentz integral transform techniques [45, 46].

Faddeev methods sum explicitly over the final states in the system, and hence are directly applicable to inclusive and exclusive responses for all possible final states. This essentially corresponds to a complete real-time calculation of the propagation of the system. Lorentz integral techniques introduce a small imaginary time component in the propagation of the response, directly summing over a limited region of  $\omega$ . For systems in which a precise calculation is possible, the full response can be calculated [46]. The Euclidean response is the fully imaginary-time response, and hence is a more integrated quantity. While detailed dynamical information is more limited, it is possible to perform calculations in much heavier systems [47].

The ground-state wave functions used in this study are obtained with variational Monte Carlo. They are of the general form [41]:

$$|\Psi_T\rangle = \prod_{i<j<k} [1 - \tilde{U}_0(ijk)] \mathcal{S} \prod_{i<j} \left[ 1 - \sum_{k \neq i,j} \tilde{U}_{2\pi}(ij;k) \right] F_{ij} |\Phi\rangle, \quad (12)$$

where for 3- and 4-nucleon systems  $|\Phi\rangle$  is simply an anti-symmetrized product of spins and isospins. The central three-nucleon correlation  $\tilde{U}_0(ijk)$  is a scaled version of the repulsive central component of the Urbana-IX (UIX) three-nucleon interaction. The magnitude of the correlation and its range are scaled via variational parameters. The pair correlations  $F_{ij}$  depend upon the pair separation  $r_{ij}$  and the spins and isospins of the pair:

$$F_{ij} = f^c(r_{ij}) \left[ 1 + u^\sigma(r) \sigma_i \cdot \sigma_j + u^t(r) S_{ij} + u^{\sigma\tau}(r) \sigma_i \cdot \sigma_j \tau_i \cdot \tau_j + u^{t\tau} S_{ij} \tau_i \cdot \tau_j \right]. \quad (13)$$

The correlation  $\tilde{U}_{2\pi}(ij;k)$  is similarly scaled from the anti-commutator part of the two-pion exchange three-nucleon interaction. The anti-commutator depends upon the spins and isospins of only the two nucleons  $i$  and  $j$ , but the spatial positions of all three. Similarly the magnitude of the spin-isospin dependent correlations  $u$  for pair  $ij$  are quenched by the presence of other nucleons. Both the two-nucleon correlation  $F_{ij}$  and the  $\tilde{U}_{2\pi}$  correlation arising from the three-nucleon interaction contain tensor-like terms correlating the spins and orientations of the nucleons. The contributions of these correlations to the response are discussed below.

While these wave functions are not exact, they offer a rather precise characterization of the Euclidean response, as evidenced by comparisons with calculations using the correlated-hyperspherical-harmonics wave functions [48] in  $A=3$ . These comparisons are presented in Sec. 9. The Hamiltonian used in these studies is the Argonne model  $v'_8$  [41] N-N interaction plus the UIX three-nucleon interaction. This interaction reproduces many known properties of the alpha particle, including its binding energy and charge form factor.

Calculation of the Euclidean response is a straightforward extension of the ground-state techniques employed in Green's function Monte Carlo. We wish to calculate matrix elements of the following type:

$$\tilde{M}(\tau) = \frac{\langle 0|O_2 \exp[-(H - E_0)\tau] O_1|0\rangle}{\langle 0|\exp[-(H - E_0)\tau]|0\rangle}. \quad (14)$$

For a ground-state calculation of the energy ( $O_1=1$ ,  $O_2=H$ ) the matrix element is evaluated by a Monte Carlo sampling of the coordinate-space paths. The denominator is exactly one for an exact ground-state wave function, otherwise there is a correction for finite  $\tau$ . For each path a complete set of  $2^A A!/(N! Z!)$  amplitudes is kept corresponding to all possible spin-isospin components of the ground state wave function. Since the operators do not in general conserve isospin we cannot use the most compact isospin basis used in ground-state calculations.

For a more general matrix element  $\tilde{M}$  we simply keep another complete set of amplitudes for each operator  $O_1$ , each set of amplitudes corresponding to the full operator acting on the ground state. The paths are sampled precisely as in the ground-state calculation [49], and hence unaffected by the operators  $O_1$ ,  $O_2$ . This allows us to calculate the response to a variety of operators (charge, current, different momenta, etc.) simultaneously.

We have found it computationally advantageous to calculate the response simultaneously for several different directions of momentum transfer. A randomly picked set of three orthogonal axes are chosen, with  $\hat{\mathbf{q}}$  directions along both the positive and negative directions of each axis. This method yields much lower statistical errors in calculating the response, and along with the more efficient methods for sampling path integrals recently applied to ground-state calculations [49], allows for much more precise results than obtained previously. It is also possible to calculate the response at several different momentum transfers simultaneously.

It is certainly possible to extract more detailed information from the Euclidean response. Most efforts in this direction proceed under Maximum Entropy techniques employing Bayesian statistics [50]. These techniques make use of the correlated error estimates in  $\tilde{R}(\tau)$  for different  $\tau$ . Given the enhanced precision of the present calculations we are exploring these possibilities. These considerations are beyond the scope of the present investigations, though, where we are primarily concerned with the total strength in the longitudinal and transverse channels.

## 5 Electromagnetic current operator

The model for the nuclear electromagnetic current adopted in the present study is briefly reviewed in this section for completeness, for a more complete description see Ref. [51]. The charge and current operators consist of one- and two-body terms:

$$\rho(\mathbf{q}) = \sum_i \rho_i^{(1)}(\mathbf{q}) + \sum_{i<j} \rho_{ij}^{(2)}(\mathbf{q}) , \quad (15)$$

$$\mathbf{j}(\mathbf{q}) = \sum_i \mathbf{j}_i^{(1)}(\mathbf{q}) + \sum_{i<j} \mathbf{j}_{ij}^{(2)}(\mathbf{q}) , \quad (16)$$

where  $\mathbf{q}$  is the momentum transfer. The one-body operators  $\rho_i^{(1)}$  and  $\mathbf{j}_i^{(1)}$  have the standard expressions obtained from a relativistic reduction of the covariant single-nucleon current, and are listed below for convenience. The charge operator is written as

$$\rho_i^{(1)}(\mathbf{q}) = \rho_{i,\text{NR}}^{(1)}(\mathbf{q}) + \rho_{i,\text{RC}}^{(1)}(\mathbf{q}) , \quad (17)$$

with

$$\rho_{i,\text{NR}}^{(1)}(\mathbf{q}) = \epsilon_i e^{i\mathbf{q}\cdot\mathbf{r}_i} , \quad (18)$$

$$\rho_{i,\text{RC}}^{(1)}(\mathbf{q}) = \left( \frac{1}{\sqrt{1 + Q^2/4m^2}} - 1 \right) \epsilon_i e^{i\mathbf{q}\cdot\mathbf{r}_i} - \frac{i}{4m^2} (2\mu_i - \epsilon_i) \mathbf{q} \cdot (\boldsymbol{\sigma}_i \times \mathbf{p}_i) e^{i\mathbf{q}\cdot\mathbf{r}_i} , \quad (19)$$

where  $Q^2 = q^2 - \omega^2$  is the four-momentum transfer, and  $\omega$  is the energy transfer. The current operator is expressed as

$$\mathbf{j}_i^{(1)}(\mathbf{q}) = \frac{1}{2m} \epsilon_i [\mathbf{p}_i , e^{i\mathbf{q}\cdot\mathbf{r}_i}]_+ - \frac{i}{2m} \mu_i \mathbf{q} \times \boldsymbol{\sigma}_i e^{i\mathbf{q}\cdot\mathbf{r}_i} , \quad (20)$$

where  $[\cdots , \cdots]_+$  denotes the anticommutator. The following definitions have been introduced:

$$\epsilon_i \equiv G_{E,p}(Q^2) \frac{1}{2} (1 + \tau_{z,i}) + G_{E,n}(Q^2) \frac{1}{2} (1 - \tau_{z,i}) , \quad (21)$$

$$\mu_i \equiv G_{M,p}(Q^2) \frac{1}{2} (1 + \tau_{z,i}) + G_{M,n}(Q^2) \frac{1}{2} (1 - \tau_{z,i}) , \quad (22)$$

and  $\mathbf{p}$ ,  $\boldsymbol{\sigma}$ , and  $\boldsymbol{\tau}$  are the nucleon's momentum, Pauli spin and isospin operators, respectively. The two terms proportional to  $1/m^2$  in  $\rho_{i,\text{RC}}^{(1)}$  are the well known Darwin-Foldy and spin-orbit relativistic corrections [52, 53], respectively.

The calculations of the response functions discussed in the previous section have been carried out using the dipole parameterization of the nucleon form factors

$$G_{E,p}(Q^2) = G_D(Q^2) , \quad (23)$$

$$G_{E,n}(Q^2) = -\mu_n \frac{Q^2}{4m^2} \frac{G_D(Q^2)}{1 + Q^2/m^2} , \quad (24)$$

$$G_{M,p}(Q^2) = \mu_p G_D(Q^2) , \quad (25)$$

$$G_{M,n}(Q^2) = \mu_n G_D(Q^2) , \quad (26)$$

where

$$G_D(Q^2) = \frac{1}{(1 + Q^2/\Lambda^2)^2} , \quad (27)$$

with  $\Lambda = 0.834$  GeV/c, and where  $\mu_p$  and  $\mu_n$  are the proton ( $\mu_p = 2.793$  n.m.) and neutron ( $\mu_n = -1.913$  n.m.) magnetic moments, respectively. It is worth emphasizing that the available semi-empirical parameterizations of the proton electric and magnetic, and neutron magnetic form factors do not differ significantly — less than a couple of %

— in the low momentum transfer range of interest here,  $Q^2 \leq 0.4$  (GeV/c)<sup>2</sup>, and that uncertainties in the neutron electric form factor have a negligible impact on the present results. Finally, we should note that in the actual calculations of the Euclidean responses the value of the four-momentum transfer occurring in the nucleon form factors (as well as in the electromagnetic  $N\Delta$  transition form factor, see below) is kept fixed at the quasi-elastic peak, as already mentioned in Sec. 4.

The most important features of the two-body parts of the electromagnetic current operator are summarized below. The reader is referred to Refs. [54, 51] for a derivation and listing of their explicit expressions.

## 5.1 Two-body current operators

The two-body current operator consists of “model-independent” and “model-dependent” components, in the classification scheme of Riska [55]. The model-independent terms are obtained [56] from the nucleon-nucleon interaction (the charge-independent part of the Argonne  $v_{18}$  in the present study), and by construction satisfy current conservation with it. The leading operator is the isovector “ $\pi$ -like” current derived from the isospin-dependent spin-spin ( $\sigma\tau$ ) and tensor ( $t\tau$ ) interactions. The latter also generate an isovector “ $\rho$ -like” current, while additional model-independent isoscalar and isovector currents arise from the isospin-independent and isospin-dependent central and momentum-dependent interactions. These currents are short-ranged and numerically far less important than the  $\pi$ -like current. For the purpose of later discussions, we list below the explicit expression for the latter:

$$\begin{aligned} \mathbf{j}_{ij}^{(2)}(\mathbf{q}; \pi) &= G_E^V(Q^2)(\tau_i \times \tau_j)_z \left[ e^{i\mathbf{q}\cdot\mathbf{r}_i} f_{PS}(r) \sigma_i (\sigma_j \cdot \hat{\mathbf{r}}) + e^{i\mathbf{q}\cdot\mathbf{r}_j} f_{PS}(r) \sigma_j (\sigma_i \cdot \hat{\mathbf{r}}) \right. \\ &\quad \left. - (\sigma_i \cdot \nabla_i)(\sigma_j \cdot \nabla_j)(\nabla_i - \nabla_j) g_{PS}(\mathbf{q}; \mathbf{R}, \mathbf{r}) \right], \end{aligned} \quad (28)$$

where  $G_E^V(Q^2) = G_{E,p}(Q^2) + G_{E,n}(Q^2)$  is the isovector combination of the nucleon electric form factors, and  $\mathbf{R}$  and  $\mathbf{r}$  are the center-of-mass and relative positions of nucleons  $i$  and  $j$ ,  $\mathbf{R} = (\mathbf{r}_i + \mathbf{r}_j)/2$  and  $\mathbf{r} = \mathbf{r}_i - \mathbf{r}_j$ , respectively. The functions  $f_{PS}$  and  $g_{PS}$  are defined as

$$f_{PS}(r) = \frac{d}{dr} \int \frac{d\mathbf{k}}{(2\pi)^3} e^{i\mathbf{k}\cdot\mathbf{r}} v_{PS}(k), \quad (29)$$

$$g_{PS}(\mathbf{q}; \mathbf{R}, \mathbf{r}) = \int \frac{d\mathbf{k}_i}{(2\pi)^3} \frac{d\mathbf{k}_j}{(2\pi)^3} e^{i\mathbf{k}_i\cdot\mathbf{r}_i} e^{i\mathbf{k}_j\cdot\mathbf{r}_j} (2\pi)^3 \delta(\mathbf{q} - \mathbf{k}_i - \mathbf{k}_j) \frac{v_{PS}(k_i) - v_{PS}(k_j)}{k_i^2 - k_j^2}, \quad (30)$$

where  $v_{PS}(k)$  is obtained from the  $\sigma\tau$  and  $t\tau$  components of the interaction,

$$v_{PS}(k) = v^{\sigma\tau}(k) - 2 v^{t\tau}(k), \quad (31)$$

with

$$v^{\sigma\tau}(k) = \frac{4\pi}{k^2} \int_0^\infty r^2 dr [j_0(kr) - 1] v^{\sigma\tau}(r) , \quad (32)$$

$$v^{t\tau}(k) = \frac{4\pi}{k^2} \int_0^\infty r^2 dr j_2(kr) v^{t\tau}(r) . \quad (33)$$

The factor  $j_0(kr) - 1$  in the expression for  $v^{\sigma\tau}(k)$  ensures that its volume integral vanishes [56].

In a one-boson-exchange (OBE) model, in which the isospin-dependent spin-spin and tensor interactions are due to  $\pi$ -meson (and  $\rho$ -meson) exchanges, the function  $v_{PS}(k)$  simply reduces to

$$v_{PS}(k) \rightarrow v_\pi(k) \equiv -\frac{f_\pi^2}{m_\pi^2} \frac{f_\pi^2(k)}{k^2 + m_\pi^2} , \quad (34)$$

where  $m_\pi$ ,  $f_\pi$ , and  $f_\pi(k)$  denote, respectively, the pion mass,  $\pi NN$  coupling constant and form factor. In this limit, the functions  $f_{PS}$  and  $g_{PS}$  read:

$$f_{PS}(r) \rightarrow f_\pi(r) = \frac{f_\pi^2}{4\pi} \frac{e^{-m_\pi r}}{(m_\pi r)^2} (1 + m_\pi r) \quad (35)$$

$$g_{PS}(\mathbf{q}; \mathbf{R}, \mathbf{r}) \rightarrow g_\pi(\mathbf{q}; \mathbf{R}, \mathbf{r}) = \frac{e^{i\mathbf{q}\cdot\mathbf{R}}}{8\pi} \int_{-1/2}^{+1/2} dx e^{-ix\mathbf{q}\cdot\mathbf{r}} \frac{e^{-L_\pi(x)r}}{L_\pi(x)} , \quad (36)$$

with

$$L_\pi(x) = \sqrt{m_\pi^2 + q^2(1 - 4x^2)}/4 , \quad (37)$$

where for simplicity the  $\pi NN$  form factor has been set equal to one. The resulting current is then identical to that commonly used in the literature.

The model-dependent currents are purely transverse and therefore cannot be directly linked to the underlying two-nucleon interaction. The present calculation includes the isoscalar  $\rho\pi\gamma$  and isovector  $\omega\pi\gamma$  transition currents as well as the isovector current associated with excitation of intermediate  $\Delta$ -isobar resonances. The  $\rho\pi\gamma$  and  $\omega\pi\gamma$  couplings are known from the measured widths of the radiative decays  $\rho \rightarrow \pi\gamma$  [57] and  $\omega \rightarrow \pi\gamma$  [58, 59], respectively, while their momentum-transfer dependence is modeled using vector-meson-dominance. Monopole form factors are introduced at the meson-baryon vertices with cutoff values of  $\Lambda_\pi=3.8 \text{ fm}^{-1}$  and  $\Lambda_\rho=\Lambda_\omega=6.3 \text{ fm}^{-1}$  at the  $\pi NN$ ,  $\rho NN$  and  $\omega NN$  vertices, respectively.

Among the model-dependent currents, however, those associated with the  $\Delta$ -isobar are the most important ones. In the present calculation, these currents are treated in the static  $\Delta$  approximation rather than in the more accurate transition-correlation-operator scheme, developed in Ref. [60] and applied to the calculation of the trinucleon form factors [61],  $nd$  and  $pd$  radiative capture cross sections at low energies [54, 62], and  $S$ -factor of the proton weak capture on  ${}^3\text{He}$  [63]. Again for later convenience, it is useful to list explicitly



the two-body  $\Delta$ -excitation current used in the present work:

$$\begin{aligned} \mathbf{j}_{ij}^{(2)}(\mathbf{q}; \Delta) = & \mathbf{j}_i(\mathbf{q}; \Delta \rightarrow N) \frac{v_{NN \rightarrow \Delta N, ij}}{m - m_\Delta} \\ & + \frac{v_{\Delta N \rightarrow NN, ij}}{m - m_\Delta} \mathbf{j}_i(\mathbf{q}; N \rightarrow \Delta) + i \rightleftharpoons j , \end{aligned} \quad (38)$$

where the  $N \rightleftharpoons \Delta$  electromagnetic current is modeled as

$$\mathbf{j}_i(\mathbf{q}; N \rightarrow \Delta) = -\frac{i}{2m} G_{\gamma N \Delta}(Q^2) e^{i\mathbf{q} \cdot \mathbf{r}_i} \mathbf{q} \times \mathbf{S}_i T_{z,i} , \quad (39)$$

and the expression for  $\mathbf{j}_i(\mathbf{q}; \Delta \rightarrow N)$  is obtained from that for  $\mathbf{j}_i(\mathbf{q}; N \rightarrow \Delta)$  by replacing the transition spin and isospin operators  $\mathbf{S}$  and  $\mathbf{T}$  with their hermitian conjugates. The electromagnetic form factor  $G_{\gamma N \Delta}(Q^2)$  is parameterized as

$$G_{\gamma N \Delta}(Q^2) = \frac{\mu^*}{(1 + Q^2/\Lambda_{N\Delta,1}^2)^2 \sqrt{1 + Q^2/\Lambda_{N\Delta,2}^2}} , \quad (40)$$

where the  $N \rightarrow \Delta$  transition magnetic moment  $\mu^*$  is taken here to be equal to 3 n.m., as obtained in an analysis of  $\gamma N$  data in the  $\Delta$ -resonance region [64]. This analysis also gives  $\Lambda_{N\Delta,1}=0.84$  GeV/c and  $\Lambda_{N\Delta,2}=1.2$  GeV/c. It is important to point out, however, that the quark-model value for  $\mu^*$ ,  $\mu^* = (3\sqrt{2}/5)\mu_N^V = 3.993$  n.m. ( $\mu_N^V$  is the nucleon isovector magnetic moment), is often used in the literature. This value is significantly larger than that adopted above. Finally, the transition interaction  $v_{NN \rightarrow \Delta N, ij}$  is given by

$$v_{NN \rightarrow \Delta N, ij} = [v^{\sigma\tau\Pi}(r) \mathbf{S}_i \cdot \sigma_j + v^{t\tau\Pi}(r) S_{ij}^{\Pi}] \mathbf{T}_i \cdot \tau_j , \quad (41)$$

and  $v_{\Delta N \rightarrow NN, ij}$  is the hermitian conjugate of the expression above. The  $S_{ij}^{\Pi}$  is the tensor operator where the Pauli spin  $\sigma_i$  has been replaced by the transition spin  $\mathbf{S}_i$ , and the functions  $v^{\sigma\tau\Pi}(r)$  and  $v^{t\tau\Pi}(r)$  are defined as

$$v^{\sigma\tau\Pi}(r) = \frac{f_\pi f_\pi^* m_\pi}{4\pi} \frac{e^{-x}}{3x} C(x) , \quad (42)$$

$$v^{t\tau\Pi}(r) = \frac{f_\pi f_\pi^* m_\pi}{4\pi} \frac{e^{-x}}{3} \left( 1 + \frac{3}{x} + \frac{3}{x^2} \right) C^2(x) , \quad (43)$$

where  $x \equiv m_\pi r$ ,  $f_\pi^* = (6\sqrt{2}/5)f_\pi$  is the quark-model value for the  $\pi N \Delta$  coupling constant (adopted in the present work), and the cutoff function  $C(x) = 1 - e^{-\lambda x^2}$ , with  $\lambda=4.09$ .

Standard manipulations of the product of spin and isospin transition operators [60] lead to the following expression for the  $\Delta$ -excitation current:

$$\begin{aligned} \mathbf{j}_{ij}^{(2)}(\mathbf{q}; \Delta) = & i \frac{G_{\gamma N \Delta}(Q^2)}{9m} e^{i\mathbf{q} \cdot \mathbf{r}_i} \left[ 4 \tau_{z,j} [f_\Delta(r) \sigma_j + g_\Delta(r) \hat{\mathbf{r}}(\sigma_j \cdot \hat{\mathbf{r}})] \right. \\ & - (\tau_i \times \tau_j)_z [f_\Delta(r) (\sigma_i \times \sigma_j) + g_\Delta(r) (\sigma_i \times \hat{\mathbf{r}})(\sigma_j \cdot \hat{\mathbf{r}})] \left. \right] \times \mathbf{q} \\ & + i \rightleftharpoons j , \end{aligned} \quad (44)$$

where

$$f_{\Delta}(r) \equiv \frac{v^{\sigma\tau II}(r) - v^{t\tau II}(r)}{m - m_{\Delta}} , \quad (45)$$

$$g_{\Delta}(r) \equiv 3 \frac{v^{t\tau II}(r)}{m - m_{\Delta}} . \quad (46)$$

The expression above reduces to that commonly used in the literature, if the quark-model values for the  $\pi N\Delta$  and  $\gamma N\Delta$  coupling constants are adopted.

## 5.2 Two-body charge operators

While the main parts of the two-body currents are linked to the form of the two-nucleon interaction through the continuity equation, the most important two-body charge operators are model-dependent, and should be considered as relativistic corrections. Indeed, a consistent calculation of two-body charge effects in nuclei would require the inclusion of relativistic effects in both the interaction models and nuclear wave functions. Such a program is yet to be carried out for systems with  $A \geq 3$ . There are nevertheless rather clear indications for the relevance of two-body charge operators from the failure of the impulse approximation (IA) in predicting the deuteron tensor polarization observable [65], and charge form factors of the three- and four-nucleon systems [61, 66]. The model commonly used [67] includes the  $\pi$ -,  $\rho$ -, and  $\omega$ -meson exchange charge operators with both isoscalar and isovector components, as well as the (isoscalar)  $\rho\pi\gamma$  and (isovector)  $\omega\pi\gamma$  charge transition couplings, in addition to the single-nucleon Darwin-Foldy and spin-orbit relativistic corrections. The  $\pi$ - and  $\rho$ -meson exchange charge operators are constructed from the isospin-dependent spin-spin and tensor components of the two-nucleon interaction (again, the Argonne  $v_{18}$  model), using the same prescription adopted for the corresponding current operators. Explicit expressions for these operators can be found in Ref. [67]. Here, we only emphasize that for  $Q \leq 1$  GeV/c the contribution due to the  $\pi$ -exchange charge operator is typically an order of magnitude larger than that of any of the remaining two-body mechanisms and one-body relativistic corrections.

## 6 Model studies

The Euclidean response is an excellent tool to test our understanding of inclusive quasi-elastic scattering, since it incorporates an exact treatment of the states in the continuum. The Euclidean response does have the disadvantage, however, that it corresponds to a weighted integral over the energy loss  $\omega$  and, as a consequence, the interpretation of potential differences between calculated results and experimental data is not so straightforward.

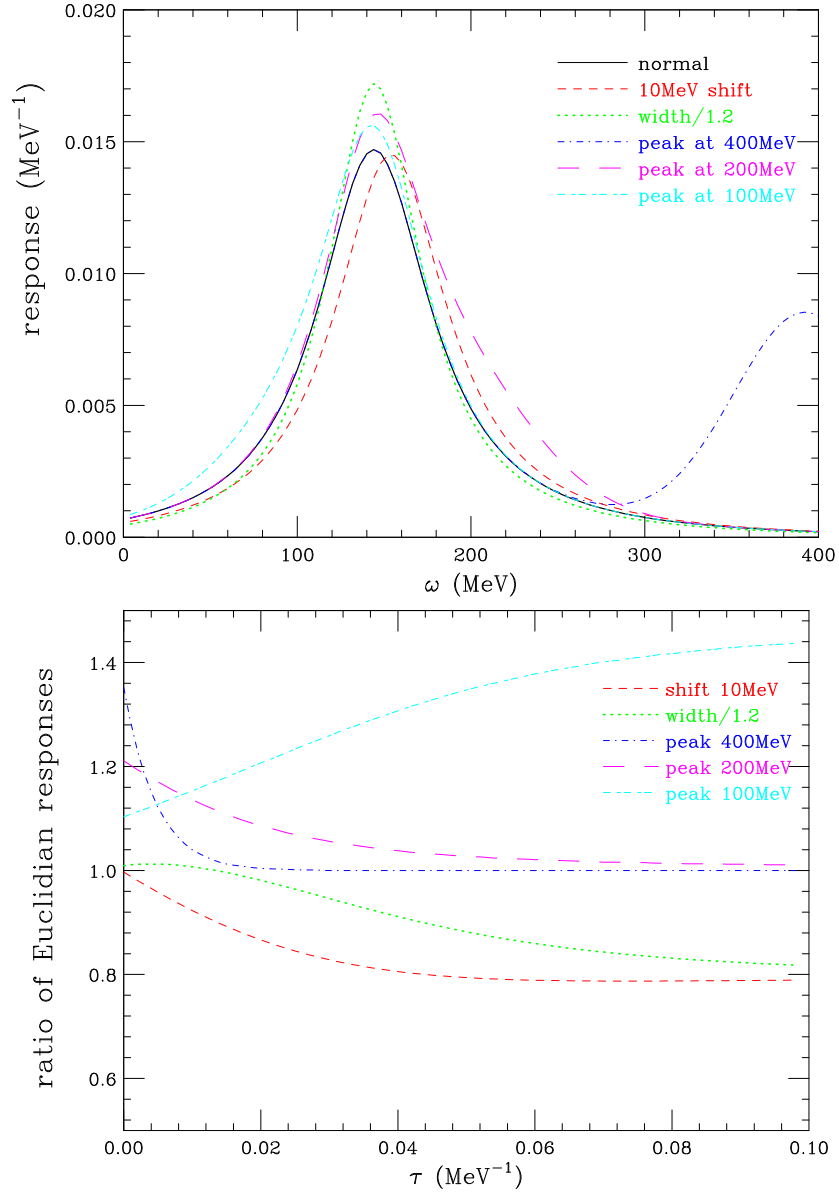


Figure 5: Top: model response (solid line) changed by various modifications (see text). Bottom: corresponding ratio of modified and unmodified Euclidian responses.

In order to develop a better feeling for the properties of the Euclidean response, in this section we discuss a simple-minded model calculation. We use a parameterized cross section — *de facto* a fit to the longitudinal  $R_L(\omega)$  at one momentum transfer — and study the change in the Euclidean response upon various changes of the cross section as a function of energy loss.

In the top panel of Fig. 5 we show the model quasi-elastic peak as a function of energy loss (solid curve) and a selection of modifications. The changes have in general been made by adding a gaussian with arbitrary amplitude and selected position in energy loss. Figure 5 shows the quasi-elastic peak a) with a gaussian placed at very large energy loss (400 MeV), b) a gaussian placed on the high-energy loss tail of the quasi-elastic peak (200 MeV) and c) a gaussian placed on the low- $\omega$  side of the peak (100 MeV). It also displays a curve where d) the width of the quasi-elastic response has been decreased by 20% (with the overall amplitude adjusted to conserve the area) and one for the case where e) the quasi-elastic peak is shifted by 10 MeV.

The lower panel of Fig. 5 shows the resulting changes in terms of the ratio of modified to original Euclidean responses. The value at  $\tau=0$  reflects the (arbitrary) integral over  $\omega$  of the added modification. Several features are noteworthy:

- The Euclidean response at finite  $\tau$  very quickly suppresses the contribution from large energy loss. The dash-dot curve shows that already at  $\tau > 0.01$  the contribution from the large peak added at  $\omega=400$  MeV is suppressed. For the experimental transverse response function  $R_T(\omega)$  this implies that the contribution from pion production in the  $\Delta$  peak (which is not included in the theory we are going to compare to) is only affecting the results for very small  $\tau$ . We will therefore ignore this region.
- The region of the quasi-elastic cross section at low  $\omega$  comes in very prominently at the larger values of  $\tau$ , as indicated by the curve labeled “peak at 100 MeV”.
- A shift of the quasi-elastic peak to larger  $\omega$  leads to an Euclidean response that quickly falls with increasing  $\tau$ , reaching saturation by the time  $\tau$  gets to values approaching 0.05.

## 7 Results

We have used the longitudinal ( $L$ ) and transverse ( $T$ ) experimental response functions of Figs. 1 and 2 to compute the corresponding experimental Euclidean responses shown in Figs. 6 and 7. The nucleon electromagnetic form factors are divided out using the parameterizations of Höhler *et al.* [68]. In order to not include too much of the tail of the  $\Delta$ -resonance, the integration has been performed up to the energy loss  $\omega$  where the  $T$ -response starts to increase significantly with  $\omega$  (the corresponding value of  $\omega$  is indicated in Figs. 1 and 2 by a +). Since for the  $T$ -Euclidean response at very small  $\tau$  the tail of the  $\Delta$ -peak nevertheless plays a role, the experimental response in this region is indicated by a dashed line only, and should not be compared to the theoretical calculations discussed below.

The statistical errors of the experimental Euclidean response are obtained via the usual error propagation when integrating. The additional overall systematic uncertainty,

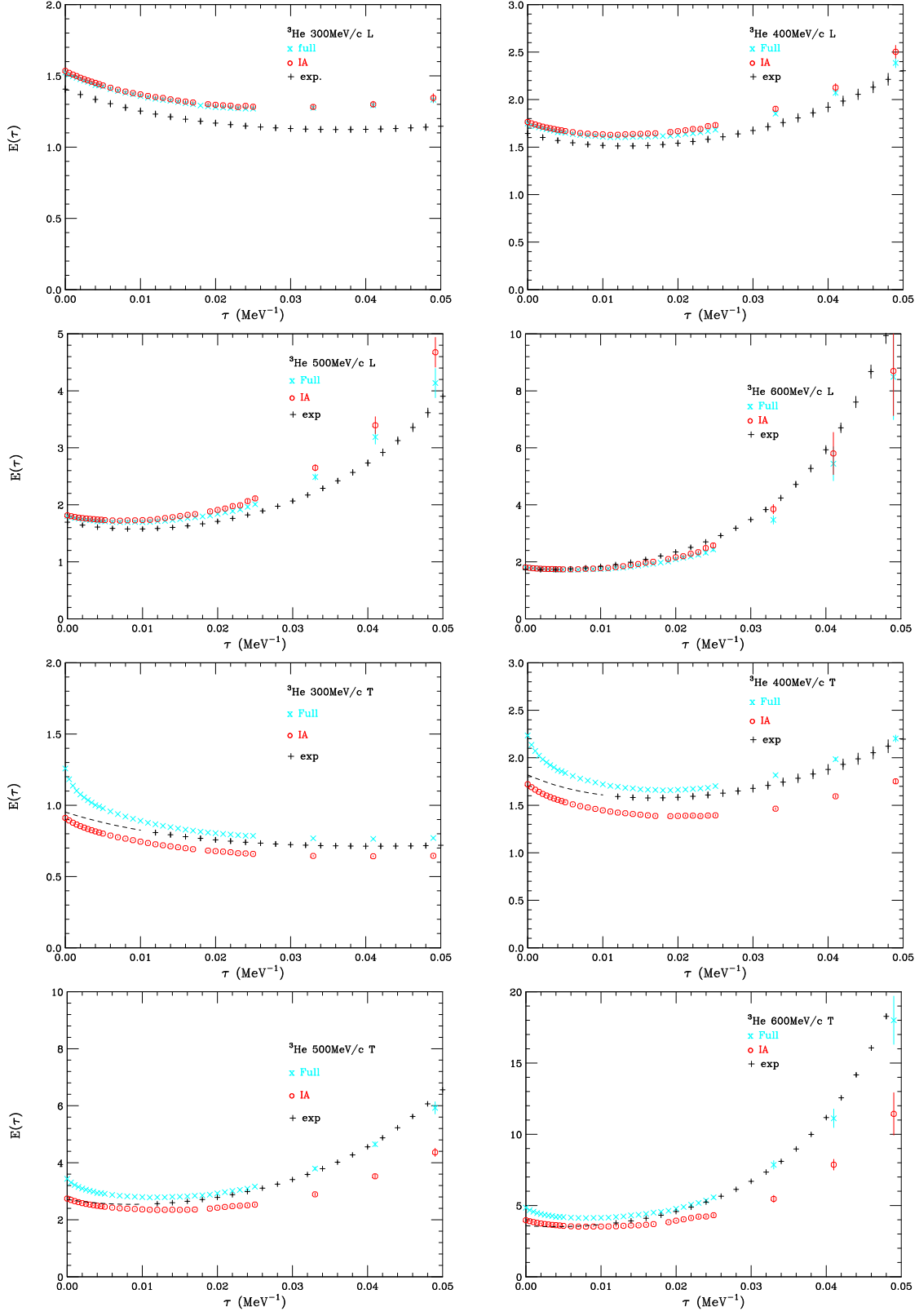


Figure 6: Longitudinal (upper half of figure) and transverse Euclidean response of  ${}^3\text{He}$  for momentum transfers 300–600 MeV/c.

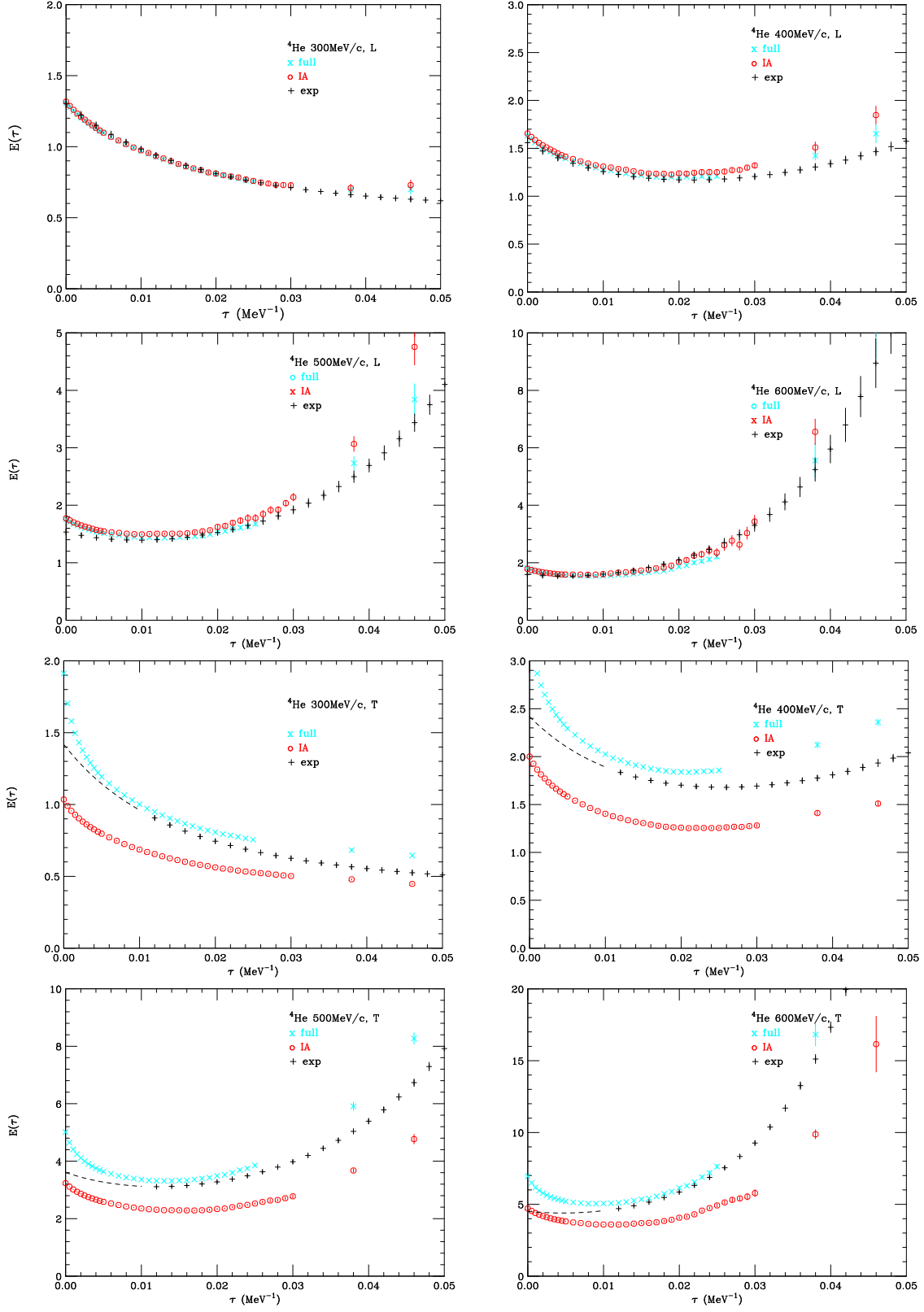


Figure 7: Longitudinal (upper half of figure) and transverse Euclidean response of  ${}^4\text{He}$  for momentum transfers 300–600 MeV/c.

estimated from the  $L/T$ -separation, amounts to typically 3% for  ${}^3\text{He}$  for both the  $L$ - and  $T$ -cross sections. For  ${}^4\text{He}$  a similar uncertainty in the scale factor applies at the lower momentum transfers and for both  $L$  and  $T$ ; at 600 MeV/c the uncertainty in  $R_L(\omega)$  increases to 6%. These scale errors, which then apply also to the corresponding Euclidean responses, have not been included in the error bars shown in Figs. 6 and 7.

In Figs. 6 and 7 we also show the calculated Euclidean responses, obtained in IA and with inclusion, in addition, of the contributions associated with the two-body charge and current operators, discussed in Sec. 5. It is immediately apparent that two-body contributions reduce by a small amount the  $L$ -responses, while increasing the  $T$ -responses very substantially at all momentum transfers. The enhancement in the  $T$ -channel occurs already at low  $\omega$ , as is seen from the Euclidean response at large  $\tau$ . Two-body effects thus are important over the entire quasi-elastic peak, and not only — as was often expected — in the “dip-region” on the large- $\omega$  side of the quasi-elastic peak. These conclusions are in agreement with those of an earlier study [21], as well as with those inferred from the super-scaling analysis of Ref. [12] for nuclei with mass number  $A=12$ –56.

When considering the effect of two-body currents as a function of momentum transfer — in particular, when studying Fig. 7 — one notes that at low  $q$  the effect of two-body currents at large  $\omega$  (low  $\tau$ ) is bigger than at low  $\omega$  (large  $\tau$ ). At large  $q$ , this situation becomes the reverse. Figures 6 and 7 also show that theory explains well the rapid increase of two-body contributions between  ${}^3\text{He}$  and  ${}^4\text{He}$ . In contrast to most published calculations (for a discussion see Sec. 1), the present calculation does give the sizeable two-body contribution required by the data.

Figure 7 shows that the  $T$ -Euclidean response at low  $q$  rises very rapidly towards very small  $\tau$ , reaching almost twice the IA value at  $\tau=0$ , thus suggesting that part of the two-body strength is located at very large  $\omega$ , basically under the  $\Delta$ -peak (compare to Fig. 5). It also implies that this strength is very spread out in  $\omega$ , and presumably best discussed in terms of the sum-rule (see Sec. 8).

At lower values of momentum transfer, the calculated  ${}^4\text{He}$   $T$ -Euclidean response is a bit high at large  $\tau$ , implying that the corresponding calculated cross section would be somewhat too high at low  $\omega$ . As emphasized by the sensitivity studies in Sec. 6, the low  $\omega$  region gets great weight for large  $\tau$ , so a small increase in the absolute value of  $\sigma(\omega)$  leads to a large increase in  $E(\tau)$ .

Overall, the agreement between theory and experiment for  ${}^4\text{He}$ , the nucleus which allows us best to study the relative role of one- and two-body contributions, is excellent for the  $L$ -response, thus implying that an accurate treatment of the nuclear spectrum has been achieved, since two-body operators give small corrections in the  $L$ -channel. For the  ${}^4\text{He}$   $T$ -Euclidean response, the large two-body effects predicted by theory are confirmed by experiment, although the associated contributions are a bit too large in the  $q$ -range 400–500 MeV/c.

## 8 Longitudinal and transverse sum rules

Sum rules provide a powerful tool for studying integral properties of the response of the nuclear many-body system to an external electromagnetic probe. Of particular interest are those for the longitudinal and transverse response functions at constant three-momentum transfers, since they can be expressed as ground-state expectation values of the charge and current operators and, therefore, do not require any knowledge of the complicated structure of the nuclear excitation spectrum. Direct comparison between the theoretically calculated and experimentally extracted sum rules cannot be made unambiguously, however, for two reasons. Firstly, the experimental determination of the longitudinal and transverse sum rules requires measuring the associated response functions in the whole energy-transfer range, from threshold up to  $\infty$ . Inclusive electron scattering experiments only allow access to the space-like region of the four-momentum transfer ( $\omega < q$ ). While the response in the time-like region ( $\omega > q$ ) could in principle be measured via  $e^+e^-$  annihilation, no such experiments have been carried out to date, to the best of our knowledge. Therefore, for a meaningful comparison between theory and experiment, one needs to estimate the strength outside the region covered by experiment. In the past, this has been accomplished, in the case of the longitudinal response, either by extrapolating the data [69] or by parameterizing the high-energy tail and using energy-weighted sum rules to constrain it [70, 71]. For the  $A=2-4$  nuclei, the unobserved strength amounts to 5–10% at the most for three-momentum transfers in the range  $q < 1$  GeV/c [71], and both procedures lead to similar results. Indeed, the calculated (non-energy-weighted) longitudinal sum rule — also known as the Coulomb sum rule — appears to be well satisfied by the data [71, 72].

The second reason that makes the direct comparison between theoretical and “experimental” sum rules difficult lies in the inherent inadequacy of the present theoretical model for the nuclear electromagnetic current, in particular its lack of explicit pion production mechanisms. The latter mostly affect the transverse response and make its  $\Delta$ -peak region outside the boundary of applicability of the present theory. The charge and current operators discussed in Sec. 5, however, should provide a realistic and quantitative description of both longitudinal and transverse response functions in the quasi-elastic peak region, where nucleon and (virtual) pion degrees of freedom are expected to be dominant. In light nuclei and at the momentum transfer values of interest here, the quasi-elastic and  $\Delta$ -production peaks are well separated, and it is therefore reasonable to study sum rules of the transverse response.

While non-energy- and energy-weighted longitudinal sum rules have been extensively studied in the past (see Refs. [51, 73] for a review), the number of studies dealing with sum rules of the transverse response is much more limited [74]. The present section focuses on the latter, in particular on the enhancement of transverse strength due to many-body components of the electromagnetic current, within the limitations discussed above. It also addresses, within the sum-rule context, the issue of the enhancement in the ratio of transverse to longitudinal strength, observed in the quasi-elastic response functions of



nuclei. Finally, it attempts to provide a semi-quantitative explanation for the observed systematics in the excess of transverse strength, both as function of mass number and momentum transfer. All the calculations are based on the AV18/UIX Hamiltonian model, and use correlated-hyperspherical-harmonics (variational Monte Carlo) wave functions for  $A=3-4$  ( $A=6$ ) nuclei.

The (non-energy-weighted) sum rules are defined as

$$\begin{aligned} S_\alpha(q) &= C_\alpha \int_{\omega_{\text{th}}^+}^{\infty} d\omega S_\alpha(q, \omega) \\ &= C_\alpha \left[ \langle 0 | O_\alpha^\dagger(\mathbf{q}) O_\alpha(\mathbf{q}) | 0 \rangle - |\langle 0 | O_\alpha(\mathbf{q}) | 0 \rangle|^2 \right] , \end{aligned} \quad (47)$$

where  $S_\alpha(q, \omega)$  is the point-nucleon longitudinal ( $\alpha=L$ ) or transverse ( $\alpha=T$ ) response function,  $O_\alpha(\mathbf{q})$  is either the charge  $\rho(\mathbf{q})$  or current  $\mathbf{j}(\mathbf{q})$  operator divided by the square of the proton form factor  $|G_E^p(\tilde{Q}^2)|^2$  (again,  $\tilde{Q}^2$  is evaluated at the energy transfer corresponding to the quasi-elastic peak),  $|0\rangle$  denotes the ground state, and the elastic contribution to the sum rule has been removed. An average over the nuclear spin orientations is tacitly implied in the evaluation of the expectation values. The constant  $C_\alpha$ , for  $\alpha=L$  or  $T$ , is given by

$$C_L = \frac{1}{Z} , \quad (48)$$

$$C_T = \frac{2m^2}{Z\mu_p^2 + N\mu_n^2} \frac{1}{q^2} , \quad (49)$$

where  $Z$  ( $N$ ) and  $\mu_p$  ( $\mu_n$ ) are the proton (neutron) number and magnetic moment, respectively. It has been introduced in Eq.(47) so that, in the limit  $q \rightarrow \infty$  and under the approximation that the nuclear charge and current operators originate, respectively, from the charge and spin-magnetization of the individual nucleons only,  $S_\alpha(q \rightarrow \infty) = 1$ . Note that the Euclidean response functions calculated in Sec. 7 and the sum rules defined here are related via

$$S_\alpha(q) = C_\alpha E_\alpha(q, \tau = 0) . \quad (50)$$

The expectation values in Eq. (47) are calculated with Monte Carlo methods, without any approximations.

The calculated sum rules for  ${}^3\text{He}$ ,  ${}^4\text{He}$ , and  ${}^6\text{Li}$  are listed in Tables 1 and 2. The longitudinal sum rule  $S_L(q)$  is relatively un-influenced by two-body charge operators, in agreement with the results of an earlier study [72]. The transverse sum rule  $S_T(q)$  is substantially increased by two-body current contributions. The resulting enhancement has two interesting features: i) it increases, for fixed  $q$ , in going from  $A=(2 \text{ to } 3)$  to 4, and decreases from  $A=4$  to 6; ii) it decreases, for fixed  $A$ , as  $q$  increases. Both these features are summarized in Figs. 8 and 9, in which the ratios  $S_T(q)/S_L(q)$ , obtained by including one-body only and both one- and two-body contributions, are plotted as function of  $A$  for fixed  $q$  and as function of  $q$  for fixed  $A$ . The former figure is reminiscent of Fig. 4, in which the ratio of transverse to longitudinal strength in the quasi-elastic region is obtained

q(MeV/c)	<sup>3</sup> He		<sup>4</sup> He		<sup>6</sup> Li	
	1	1+2	1	1+2	1	1+2
300	0.787	0.763	0.670	0.649	0.977	0.933
400	0.921	0.875	0.859	0.815	0.995	0.932
500	0.964	0.901	0.941	0.881	0.990	0.921
600	0.982	0.908	0.973	0.910	0.990	0.924
700	0.994	0.914	0.994	0.942	0.994	0.938

Table 1: The longitudinal sum rule obtained with one-body only and both one- and two-body charge operators.

q(MeV/c)	<sup>3</sup> He		<sup>4</sup> He		<sup>6</sup> Li	
	1	1+2	1	1+2	1	1+2
300	0.929	1.31	0.893	1.67	0.912	1.57
400	0.987	1.30	0.970	1.62	0.974	1.52
500	1.01	1.28	1.00	1.55	0.999	1.46
600	1.01	1.25	1.01	1.49	1.01	1.41
700	1.01	1.23	1.01	1.44	1.011	1.37

Table 2: The transverse sum rule obtained with one-body only and both one- and two-body current operators.

from the measured response functions. Obviously, the truncated integrals in Fig. 4 do not include the strength at high  $\omega$ .

The purpose of the present section is to offer an explanation of the features mentioned above. To this end, three points are worth emphasizing. Firstly, among the two-body current contributions, the most important are those associated with the *PS* (pion-like) and  $\Delta$ -excitation currents. This fact has been explicitly verified by direct calculation, as shown in Table 3 for <sup>4</sup>He, as an example. Note that the results in the 2nd and 3rd columns are slightly different from those reported above in Table 2, since they are based on a random walk consisting only of 1,000 configurations, much shorter than that used in the calculations of Table 2. These calculations, though, are based upon the same random walk and therefore allow a better determination of the individual contributions.

Secondly, consider expanding the current into one- and two-body components  $j_l$  and  $j_{lm}$ ,

$$j = \sum_l j_l + \sum_{l < m} j_{lm} . \quad (51)$$

Then, ignoring the very small (and, with increasing  $q$ , rapidly vanishing) elastic contri-

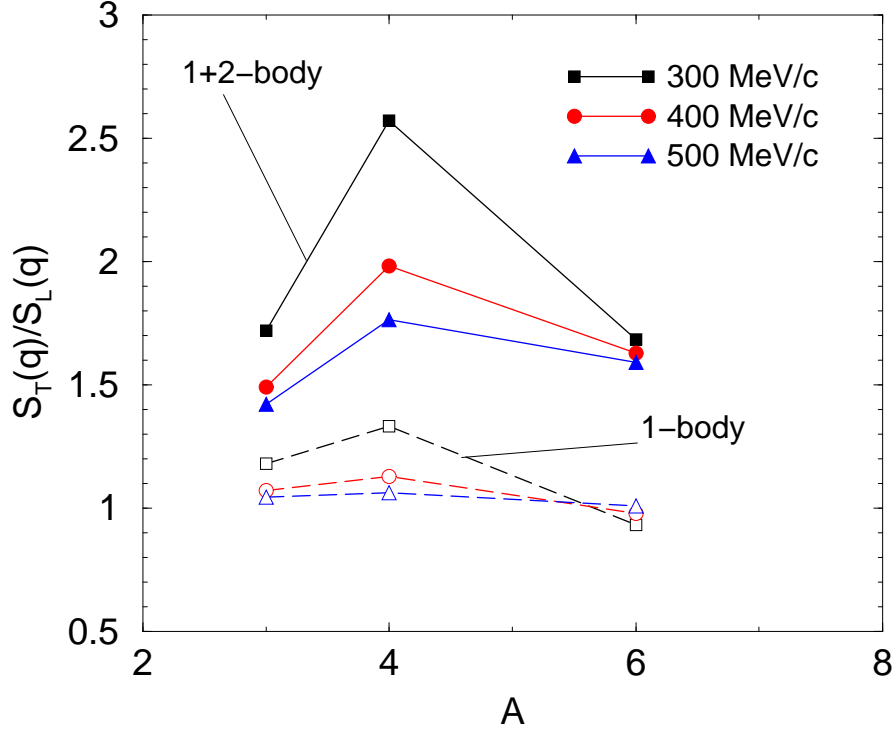


Figure 8: The ratios  $S_T(q)/S_L(q)$ , obtained with one-body currents only and both one- and two-body currents, as function of mass number  $A$ .

$q(\text{MeV}/c)$	1	1+2	1+2- $\pi$ +2- $\Delta$
300	0.915	1.65	1.58
400	0.980	1.59	1.50
500	1.01	1.53	1.44
600	1.01	1.47	1.38
700	1.01	1.41	1.33

Table 3: The  ${}^4\text{He}$  transverse sum rule.

tribution to  $S_T(q)$ , one finds that the first term in Eq. (47)

$$\begin{aligned}
 j^\dagger j &= \sum_l j_l^\dagger j_l + \sum_{l \neq m} j_l^\dagger j_m \\
 &+ \sum_{l < m} [(j_l^\dagger + j_m^\dagger) j_{lm} + \text{h.c.}] + \sum_{l < m} j_{lm}^\dagger j_{lm} \\
 &+ \text{terms involving 3 or 4 different nucleons} . \tag{52}
 \end{aligned}$$

At large momentum transfers, one would expect terms involving 3 or 4 nucleons to be

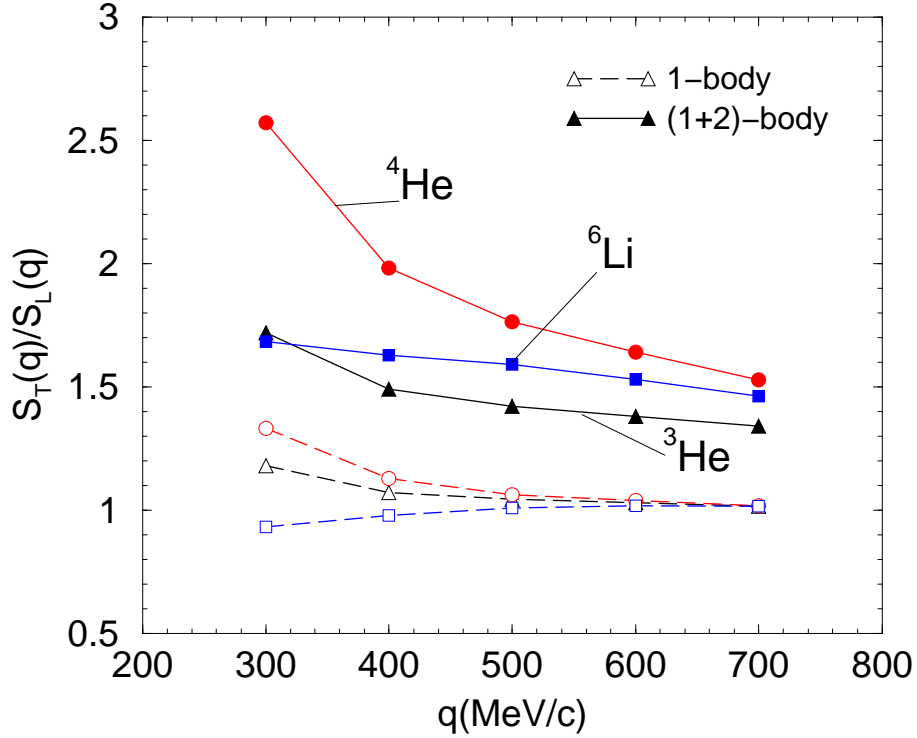


Figure 9: The ratios  $S_T(q)/S_L(q)$ , obtained with one-body currents only and both one- and two-body currents, as function of momentum transfer  $q$ .

small, particularly in light nuclei where Pauli correlations are unimportant. Dropping the last term corresponds to considering only incoherent scattering from pairs of nucleons.

This simple expectation is indeed borne out by a direct calculation, the results of which are listed for  ${}^4\text{He}$  in Table 4. Thus the transverse sum rule appears to be saturated by the one- and two-body terms in the expansion for  $j^\dagger j$  above.

$q(\text{MeV}/c)$	1	1+2	1+2-reduced
300	0.915	1.65	1.70
400	0.980	1.59	1.59
500	1.01	1.53	1.51
600	1.01	1.47	1.45
700	1.01	1.41	1.39

Table 4: The  ${}^4\text{He}$  transverse sum rule: effect of three- or four-nucleon terms.

Thirdly, the transverse strength associated with two-body currents is almost entirely

due to  $pn$  pairs. To make this observation more precise, consider the “reduced” two-body current:

$$j_{lm} \rightarrow j_{lm}(P_l P_m + N_l N_m) , \quad (53)$$

where  $P_l$  and  $N_l$  are the proton and neutron projection operators for particle  $l$ . Thus the “reduced” two-body current only acts on  $pp$  or  $nn$  pairs, and the transverse sum rule calculated with it should be given almost entirely by the one-body part of  $j$ . This fact is again confirmed by direct calculation, as it is evident from Table 5. That  $pn$  pairs

q(MeV/c)	1	1+2	1+2- $pp$ or $nn$ only
300	0.915	1.65	0.919
400	0.980	1.59	0.987
500	1.01	1.53	1.02
600	1.01	1.47	1.03
700	1.01	1.41	1.03

Table 5: The  ${}^4\text{He}$  transverse sum rule: contribution of  $pp$  and  $nn$  pairs.

are responsible for the strength due to two-body currents can also be understood by the following considerations. The pion-like and  $\Delta$ -excitation currents have the isospin structure (see Sec. 5), again in a schematic notation,

$$j_{lm}(\pi) = (\tau_l \times \tau_m)_z O_{lm}(\pi) , \quad (54)$$

$$j_{lm}(\Delta) = \tau_{l,z} O_{lm}(\Delta, a) + \tau_{m,z} O_{ml}(\Delta, a) + (\tau_l \times \tau_m)_z O_{lm}(\Delta, b) , \quad (55)$$

while the leading part of the one-body current is given by

$$j_l = \tau_{l,z} O_l(IV) , \quad (56)$$

where  $O_l(IV)$  denotes the isovector part of  $j_l$ . Now the term  $j_{lm}^\dagger j_{lm}$  (with  $j_{lm}$  including pion-like and  $\Delta$ -excitation currents) will produce, as far as isospin is concerned, terms like

$$(\tau_l \times \tau_m)_z^2 = 2(1 - \tau_{l,z} \tau_{m,z}) , \quad (57)$$

$$(\tau_{l,z} \text{ or } \tau_{m,z})(\tau_l \times \tau_m)_z = \pm i(\tau_l \cdot \tau_m - \tau_{l,z} \tau_{m,z}) , \quad (58)$$

$$\tau_{l,z} \tau_{m,z} = \frac{T_{lm} + \tau_l \cdot \tau_m}{3} , \quad (59)$$

where  $T_{lm}$  is the isotensor term  $T_{lm} = 3\tau_{l,z} \tau_{m,z} - \tau_l \cdot \tau_m$ .

In addition, there will also be isospin-independent terms, of the type

$$O_{lm}^\dagger(\Delta, a) O_{lm}(\Delta, a) . \quad (60)$$

However, it is important to note that the operators in Eqs. (57) and (58) vanish when acting on  $pp$  or  $nn$  pairs. It should also be noted that the isotensor term in Eq. (59)

vanishes in  $T=0$  and  $T=1/2$  ground states, namely in  ${}^3\text{He}$ ,  ${}^4\text{He}$  and  ${}^6\text{Li}$ . A similar analysis can be carried out for the interference terms between one- and two-body currents,

$$\sum_{l<m} (j_l^\dagger + j_m^\dagger) j_{lm} + \text{h.c.} , \quad (61)$$

for which one obtains isospin-independent, and type (58) or type (59) operators. In any case, the direct calculation indicates (see Table 5) that  $pp$  and  $nn$  pairs do not contribute appreciably to  $S_T(q)$ .

On the basis of the above observations and ignoring the convection term in the one-body  $j_l$ , one concludes that the excess transverse strength, defined as

$$\Delta S_T(q) \equiv S_T(q) - S_T(q; 1\text{-body}) , \quad (62)$$

must be proportional to

$$\Delta S_T(q) = \int_0^\infty dx \text{tr}[F(x; q) \rho(x; pn)] , \quad (63)$$

where  $F(x; q)$  is a complicated matrix in the spin-space of the two nucleons depending upon the current operators alone, and the  $A$ -dependence is included in the  $pn$  elements of the two-nucleon density matrix  $\rho_2(x; pn, s_l, s_m, s'_l, s'_m)$ . Here  $s_l, s_m$ , etc., are spin projections (up or down) of particles  $l, m$ , etc. In fact, one can express these densities in terms of total spin-isospin  $S, T=0,1$  or  $1,0$  for pair  $lm$ . The crucial point is that, in nuclei, these  $pn$  densities scale, see [75], namely

$$\rho_2(x; T = 0; A) = R_A \rho(x; T = 0; \text{deuteron}) , \quad (64)$$

$$\rho_2(x; T = 1; A) = R'_A \rho(x; T = 1; {}^1S_0 \text{ quasi-bound}) . \quad (65)$$

The scaling factors  $R_A$  and  $R'_A$  have been calculated in Ref. [75], with  $R'_A \simeq R_A$  and  $R_A=2.0, 4.7, 6.3, 18.8$  for  ${}^3\text{He}, {}^4\text{He}, {}^6\text{Li}$ , and  ${}^{16}\text{O}$ , respectively, and so one would expect  $\Delta S_T(q)$  to scale with

$$\Delta S_T(q) \propto \frac{R_A}{Z\mu_p^2 + N\mu_n^2} , \quad (66)$$

where the factor in the denominator on the r.h.s. is from the normalization adopted for  $S_T(q)$ .

The calculated values for the excess strength  $\Delta S_T(q)$  are listed in Table 6. On the basis of the scaling law above one would deduce

$$\frac{\Delta S_T(q; {}^4\text{He})}{\Delta S_T(q; {}^3\text{He})} \simeq 0.840 \frac{R_4}{R_3} = 1.97 , \quad (67)$$

$$\frac{\Delta S_T(q; {}^6\text{Li})}{\Delta S_T(q; {}^4\text{He})} \simeq 0.667 \frac{R_6}{R_4} = 0.894 , \quad (68)$$

q(MeV/c)	<sup>3</sup> He	<sup>4</sup> He	<sup>6</sup> Li
300	0.38	0.78	0.66
500	0.27	0.55	0.46
700	0.21	0.43	0.36

Table 6: The excess strength  $\Delta S_T(q)$  calculated in <sup>3</sup>He, <sup>4</sup>He, and <sup>6</sup>Li.

and these values are reasonably close to those of Table 6. They are also close to those that can be inferred from data, see Fig. 4. Finally, in Fig. 10 the integrands in Eq. (63) are displayed for <sup>3</sup>He, <sup>4</sup>He, and <sup>6</sup>Li, properly scaled according to the factor in Eq. (66). Note that also shown are the contributions due to  $pn$  pairs in  $T=0$  states only. The behavior of the integrands, as illustrated in Fig. 10, is to be expected, since it is a consequence of the “scaling” behavior more generally observed for the calculated  $T, S=0,1$  and  $1,0$  pair-distribution functions in nuclei [75].

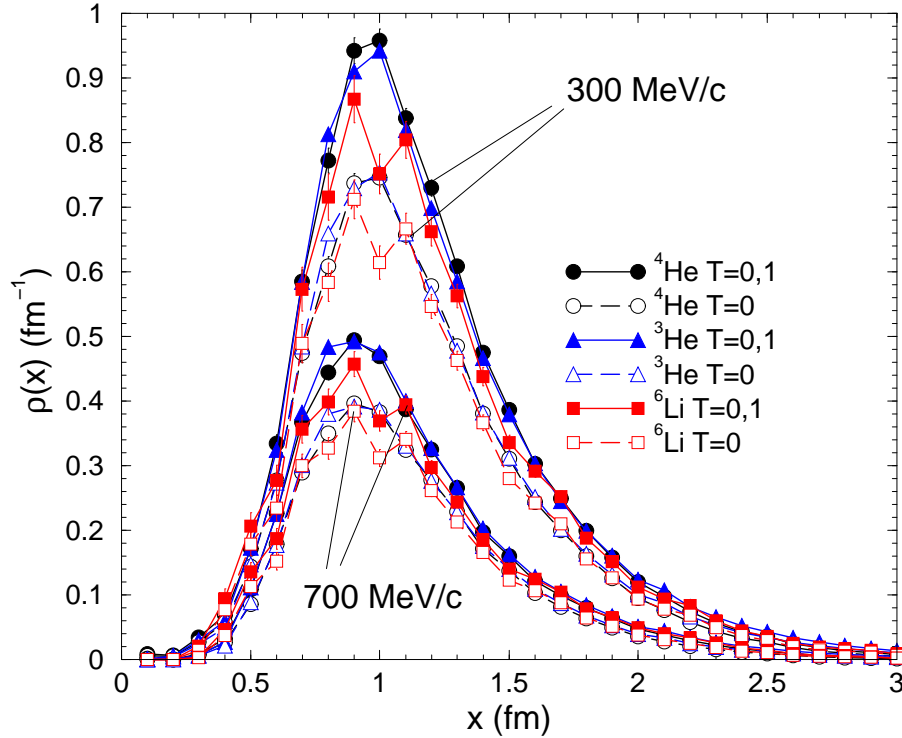


Figure 10: The integrands in Eq.(63) for <sup>3</sup>He, <sup>4</sup>He, and <sup>6</sup>Li at momentum transfers of 300 and 700 MeV/c, scaled according to the factor in Eq. (66). Also shown are the contributions due  $pn$  pairs in  $T=0$  states only.

Note that the dominant contributions to the excess strength occur for pair separations

around or slightly less than one fermi. One would naturally associate this strength with a significant contribution to two-nucleon final states of relatively large relative momenta. Detailed microscopic calculations in  $A=4$  with full final-state interactions and two-body currents will be necessary to make precise predictions.

It should be emphasized that the scaling law for  $\Delta S_T(q)$  can be used to estimate the excess transverse strength in nuclei, once the factors  $R_A$  are known. In nuclear matter, for example, the authors of Ref. [76] obtain  $R_\infty = 1.59$ , the latter being defined as  $R_A/A$  in the limit  $A \rightarrow \infty$ , and therefore one would expect a very substantial enhancement of the transverse sum rule (and, consequently, transverse response function) due to two-body currents, namely  $\Delta S_T(q; \infty)/\Delta S_T(q; {}^4\text{He}) \simeq 1.35$ .

The nuclear matter transverse response has been calculated in Ref. [77], by using correlated-basis-function perturbation theory and including, in addition to the single-nucleon spin-magnetization current, the pion-like and  $\Delta$ -excitation two-body currents. Explicit integration of the response functions [77, 78] indicates that the transverse strength is increased by the two-body contributions by roughly 15% in the momentum transfer range 300–700 MeV/c. This enhancement is significantly smaller than that inferred from the scaling law above. The underestimate is presumably due to the inherent limitations in the calculations carried out so far, which only retained one-particle–one-hole ( $1p$ - $1h$ ) intermediate states and estimated the contribution of two-particle–two-hole states by folding the  $1p$ - $1h$  response with a width derived from the imaginary part of the optical potential. It should be possible to calculate the transverse sum rule by direct evaluation of the ground state expectation value. Work along these lines is in progress [78].

The longitudinal and transverse sum rules in matter can be estimated in a Fermi gas model in a similar simple manner. As in calculations of  ${}^4\text{He}$  (see Sec. 9), this is useful to help understand the role of initial-state correlations in the transverse response of the nucleus. We again ignore contributions of 3 and 4 nucleon terms as in Eq. 52. In matter this approximation should be valid at high momentum transfer  $q$ , but becomes more questionable as  $q$  is decreased. A significant enhancement of the transverse sum rule is expected due to the short-range part of the two-body currents — these necessarily involve large momenta between the pair of nucleons, thus broadening the range of validity of this simple approximation.

The Fermi-gas sum rules are decomposed into parts depending only on the single nucleon currents and the remaining terms which also involve two-nucleon currents:

$$S_\alpha(q) = S_\alpha(q; 1\text{-body}) + \Delta S_\alpha(q) , \quad (69)$$

where  $\alpha=L, T$ . The simplest approximation to the response due to one-body currents is to assume incoherent scattering from isolated nucleons. This yields  $S_\alpha(q) = 1$ , neglecting the neutron charge and convection current contributions to the longitudinal and transverse response functions, respectively.

The additional contributions to the sum rules involving two-nucleon currents can be written as a sum of interference terms between one- and two-nucleon operators and the



square of the two-nucleon operators, in the same approximation adopted above. The short-range nature of the two-nucleon operators implies that incoherent scattering from pairs of nucleons should be dominant:

$$\Delta S_\alpha(q) = (A - 1)[2 \langle \Phi | [O_{\alpha,l}^\dagger(\mathbf{q})O_{\alpha,lm}(\mathbf{q}) + \text{h.c.}] + O_{\alpha,lm}^\dagger(\mathbf{q})O_{\alpha,lm}(\mathbf{q}) | \Phi \rangle] , \quad (70)$$

where the factor 2 in the interference term arises because the pair term can connect to either of the two single-nucleon operators.

To make a simple estimate of the contribution of the two-nucleon terms of the current, we consider the two-nucleon density matrix  $\rho_2(r_{lm})_{\chi,\chi'}$ , which depends only upon the separation between the pair of nucleons and upon their initial and final spins and isospins  $\chi$  and  $\chi'$ . In the Fermi gas approximation,  $\rho_2$  is diagonal in the spins and isospins, and the spatial dependence is given by simple Slater functions. We then obtain:

$$\Delta S_\alpha(q) = \rho \sum_{\chi,\chi'} \int d\mathbf{r}_{ij} \int \frac{d\Omega_{\hat{\mathbf{q}}}}{4\pi} \rho_2(r_{ij})_{\chi,\chi'} \langle \chi | [2 O_{\alpha,l}^\dagger(\mathbf{q}) + O_{\alpha,lm}^\dagger(\mathbf{q})] O_{lm}(\mathbf{q}) | \chi' \rangle , \quad (71)$$

where momentum-dependent pieces in the current have again been dropped. The excess contributions involving two-nucleon currents are given in Table 7 for the Fermi gas model. The longitudinal contributions are positive but small, ranging up to  $\simeq 0.02$ . The transverse contributions, ranging from  $\simeq 0.06$  at 700 MeV/c to  $\simeq 0.11$  at 300 MeV/c, are significant.

Finally, as far as the  $q$ -dependence is concerned, from the explicit expressions of the current operators in Sec. 5 it is evident that the excess transverse strength should behave as

$$\Delta S_T(q) \simeq (\alpha + \beta q + \gamma q^2)/q^2 , \quad (72)$$

where the  $q^2$ -factor in the denominator is due to the normalization adopted for  $S_T(q)$ , and so will approach a constant in the limit of large  $q$ .

q (MeV/c)	$\Delta S_L$	$\Delta S_T$
300	0.004	0.114
400	0.007	0.081
500	0.011	0.066
600	0.017	0.060
700	0.024	0.056

Table 7: Excess-strength contributions  $\Delta S_L$  and  $\Delta S_T$  to the Fermi gas sum rules from terms involving two-nucleon currents.

## 9 Model studies with simplified interactions, wave functions, and currents

As a guide to better understanding these results and comparing with other calculations, it is useful to contrast the complete calculations described above with various truncations of the initial ground state wave function, the current operators, and the Hamiltonian. Of course only the complete calculations can be meaningfully compared to the data, as they include both initial state wave functions and current operators which are consistent with the Hamiltonian used to determine the  $\tau$ - (or energy-) dependence of the response.

The transverse channel is most interesting in this regard, as it shows a large enhancement from the two-nucleon current operators. Results for  ${}^4\text{He}$  at 400 MeV/c with various truncations are shown in Fig. 11. The truncations include full (FW) and simple (SW) wave functions, full (FC) and impulse (IC) currents, and full (FI) and simple (SI) interactions. The simple wave functions and interactions are described below. The differences in the longitudinal channel are much less dramatic.

The full ground-state variational wave function is described above (Eq. 12), it includes strong tensor correlations from the pair correlation operators  $F_{ij}$  and from the three-nucleon correlation  $\tilde{U}_{2\pi}$ . In order to better determine the origin of the enhancement arising from the two-body currents, we have also considered a simplified ground-state wave function (SW) where the tensor correlations  $u^t(r)$  and  $u^{t\tau}(r)$  (Eq. 13)) and the  $\tilde{U}_{2\pi}$  correlations arising from the two-pion-exchange three-nucleon interaction have been set to zero.

Similarly it is interesting to compare the effect of different Hamiltonians describing the final-state interactions. In the Euclidean response this corresponds to using different Hamiltonians for the imaginary-time propagation of the system. The Hamiltonian used in the propagation does not directly affect the sum rules which depend only upon the initial state and the current operators. We have constructed a simplified  $v_4$  interaction (SI) where the tensor terms in the full Hamiltonian have been set to zero. This would, of course, yield a very under-bound alpha-particle ground-state. To compensate, we add a potential of two-pion exchange range to both the spin one channels:

$$v'_{S=1;T=0,1}(r) = v_{S=1;T=0,1}(r) - 1.4 T_\pi^2(r) , \quad (73)$$

where

$$T_\pi(r) = [1 - \exp(-cr^2)]^2 \left[ 1 + \frac{3}{\mu r} + \frac{3}{(\mu r)^2} \right] \frac{\exp(-\mu r)}{r} \quad (74)$$

is taken from the Argonne interaction models and is a function of two-pion exchange range. The constant 1.4 MeV-fm has been set to crudely reproduce the alpha-particle binding. This allows us to concentrate on the spin-dependence of the final-state interactions as opposed to drastically altering the spectra of the struck nucleus. In all cases the full currents (FC) are those obtained from the Argonne  $v_{18}$  interaction (AV18), they have not

been reconstructed to be consistent with the Hamiltonian used for the initial- or final-states. The motivation here is to examine the various contributions to the full calculation.

From the figure it is clear that a dramatic difference remains between full (FC) and impulse (IC) currents whatever model is chosen for the wave function and Hamiltonian. The  $\tau = 0$  (sum-rule) difference between full and impulse currents is largest for the full wave function, but even with a highly simplified wave function (SW) a large difference remains between the results with full currents (FC, SW) and impulse currents alone (IC, SW).

On the basis of Fermi-gas calculations of matter, it had been believed that the large enhancement from two-body currents found in previous calculations of light nuclei[21] were due to the presence of strong tensor correlations in the ground-state wave function. While these correlations do make a significant contribution, even simplified wave functions show a substantial enhancement. In light nuclei, at least, this is a consequence of the complete set of final states automatically included in the sum rule and Euclidean response calculations. We have also considered more drastic simplifications for the ground-state wave function, including only central ( $f^c$ ) correlations. Even in this case there is a dramatic enhancement of the response when two-nucleon currents are included.

Of course the Hamiltonian used for final-state interactions cannot affect the sum rule at  $\tau=0$ , but it can change the energy-dependence of the response. Calculations with simple wave functions (SW) and the simplified interactions (SI) are shown as diamonds in the figure. With simplified wave functions, interactions and impulse currents (IC, SW, SI), the slope at  $\tau=0$  is much more shallow corresponding to an energy-weighted sum rule much closer to  $k^2/(2m)$  than in the full calculation — of course, this is to be expected, since tensor components, missing in the SI model, substantially enhance the energy-weighted sum rule. This same interaction also has a larger low-energy (large- $\tau$ ) response than the calculations made with the full current. This is undoubtedly related to the choice of modified Hamiltonian, the choice made here will be more attractive in p-waves than the full Hamiltonian, and these presumably dominate the low-energy transverse response in  ${}^4\text{He}$ .

With the full currents (FC), there is much less dependence upon the choice of final-state interactions. Indeed, the calculations with the simple wave function and full currents (FC, SW) are nearly identical over the range of  $\tau$  considered. The low-energy p-wave continuum in the more attractive simplified Hamiltonian yields less overlap with the two-nucleon current operators, resulting in a very similar full response for the two different final-state interactions. The full calculation (FC, FW, FI) has a much larger contribution at higher energy, resulting in a steep initial fall-off with  $\tau$ . It also has a somewhat smaller response at low energy (large  $\tau$ ) than the full calculation.

Finally, we have calculated the responses in  $A=3$  using the correlated-hyperspherical-harmonics (CHH) wave functions obtained by the Pisa group [48] for this same Hamiltonian. Calculations of the longitudinal response of  ${}^3\text{He}$  at various momentum transfers are

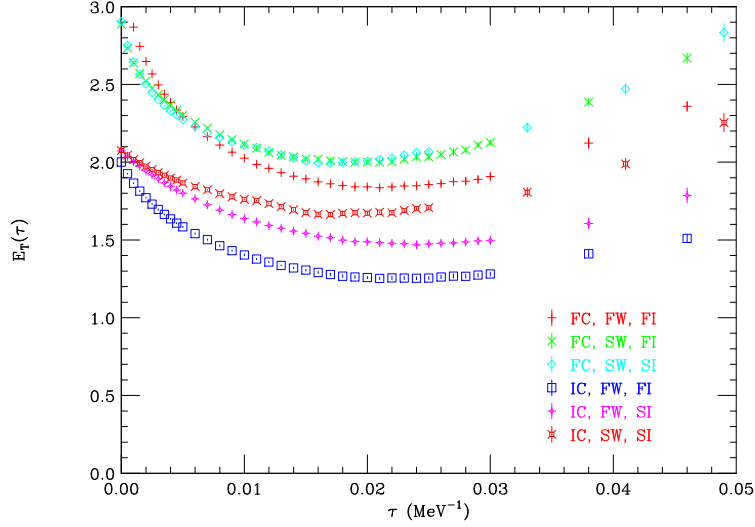


Figure 11: Euclidean transverse response for  ${}^4\text{He}$  at 400 MeV/c with full (F) or IA (I) current (C), full or simplified (S) wave function (W), full or simplified interaction (I).

compared in Fig. 12. The differences between the variational and CHH wave functions are very small, as is apparent in the figure. This is perhaps not surprising, as the drastic truncations made in the comparisons of simple (SW) and full (FW) variational wave functions were themselves somewhat modest. Differences in the CHH and VMC transverse response calculations of  ${}^3\text{He}$  are also quite small.

These calculations demonstrate that the two-nucleon currents play a crucial role in the transverse response. Precise comparisons with experimental data also require calculations with accurate initial-state wave functions and final-state interactions. In such realistic calculations, the contributions of the two-nucleon currents are large both in the integrated response and in the low- $\omega$  regime.

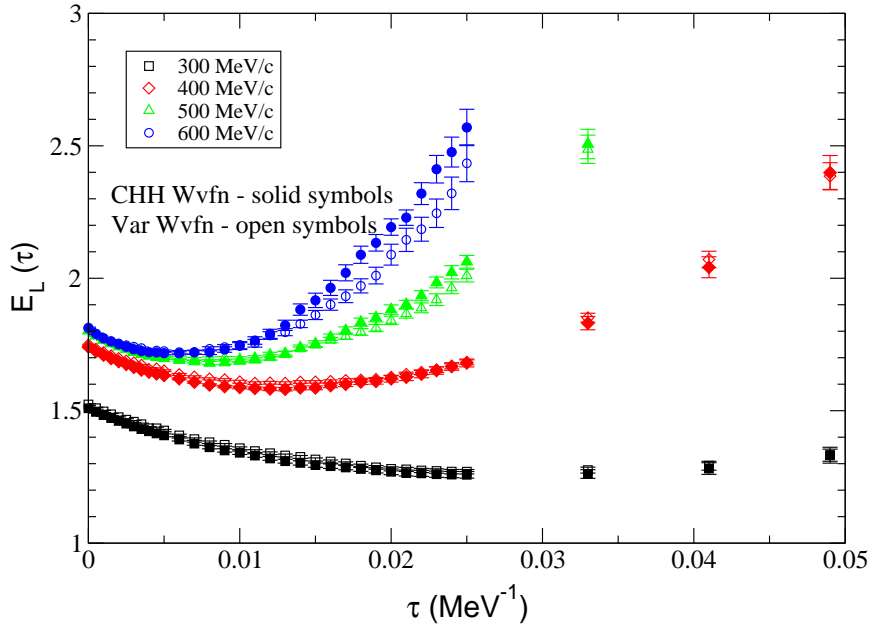


Figure 12: Comparison of the  ${}^3\text{He}$  Euclidean longitudinal response functions using variational (open symbols) and CHH (solid symbols) wave functions.

## 10 Conclusions

We have determined the  ${}^3\text{He}$  and  ${}^4\text{He}$  longitudinal and transverse response functions in the momentum transfer range 300–700 MeV/c from an analysis of the  $(e,e')$  world data. The corresponding Euclidean response functions have been derived by direct Laplace transform of the experimental data, and have been found to be in satisfactory agreement with those calculated with Green’s function Monte Carlo methods using realistic interactions and currents. Leading terms of the two-body charge and current operators are constructed consistently with the two-nucleon interaction included in the Hamiltonian (the Argonne  $v_{18}$ ). A number of improvements in the algorithms employed for the Monte Carlo evaluation of the relevant path integrals have allowed us to reduce, very significantly, the statistical errors in the Euclidean response calculations.

Two-body charge operators reduce slightly the one-body longitudinal strength at large  $\tau$  (corresponding to the threshold region of  $R_L(q,\omega)$ ), while two-body currents increase very substantially, and particularly for  ${}^4\text{He}$ , the one-body transverse strength over the whole  $\tau$ -range considered. Thus, in the quasi-elastic region, single-nucleon knock-out processes are dominant in the longitudinal channel, while both one- and two-body mechanisms contribute with comparable magnitude in the transverse channel. These qualita-

tive conclusions are corroborated by the scaling analysis of the data described in Sec. 3: the longitudinal and transverse scaling functions  $f_L$  and  $f_T$ , which would be expected to overlap if one-body processes alone were to be at play, display in fact drastically different trends (see Fig. 3). The enhancement in the ratio of transverse to longitudinal quasi-elastic strength can be quantified by considering integrals of  $f_L$  and  $f_T$  (of course, over the quasi-elastic peak region alone), as done in Fig. 4. Experimentally, this  $T/L$  ratio is found to increase very significantly from  $A=3$  to 4, to decrease only moderately from  $A=4$  to 12, and to remain rather flat as  $A=12$ –56. Of course, the interpretation of the integral of  $f_T$  as reflecting exclusively quasi-elastic strength is not entirely correct, particularly since, as the momentum transfer becomes larger and larger, the quasi-elastic and  $\Delta$  peaks tend to merge together: strength from the pion-production region will then necessarily spill over into the quasi-elastic region, contaminating  $f_T$ . Nevertheless, the amount of “spurious” (non quasi-elastic) strength contamination should not be too large, at least for light nuclei, for which the quasi-elastic and  $\Delta$  peaks remain well separated at all momentum transfers considered here. The observed enhancement of the  $T/L$  ratio in  ${}^3\text{He}$  and  ${}^4\text{He}$  is well reproduced by theory, since the Euclidean response functions derived from data are close to those obtained in the calculations, over the whole  $\tau$ -range.

The  $T/L$  ratio has also been studied in the  $A=3$ , 4, and 6 nuclei via sum-rule techniques. Even within the limitations that such an approach necessarily entails (see Sec. 8), there are rather clear indications that the present theory is able to predict its observed dependence upon both mass number and momentum transfer, see Figs. 8 and 9. The sum rule study in Sec. 8 has also allowed us to establish quantitatively that the excess transverse strength associated with two-body currents is almost entirely due to  $pn$  pairs. This fact has then led to the scaling law for the excess transverse strength  $\Delta S_T(q) \simeq R_A/A$ , which derives from the universal scaling behavior obtained for the calculated  $pn$ -pair distribution functions in nuclei [75].

Finally, the role of tensor interactions and correlations has been investigated via model studies of the  ${}^4\text{He}$  Euclidean transverse response function, using simplified interactions, currents, and wave functions. In contrast to earlier speculations [21] that the large enhancement from two-body currents was due to the presence of strong tensor correlations in the ground state, it is now clear that this enhancement arises from the concerted interplay of tensor interactions and correlations in both ground and scattering states. A successful prediction of the longitudinal and transverse response functions in the quasi-elastic region demands an accurate description of nuclear dynamics, based on realistic interactions and currents.

## Acknowledgments

We wish to thank R.B. Wiringa for allowing us to use his variational Monte Carlo wave functions, and A. Kievsky, S. Rosati, and M. Viviani for providing us with their correlated-

hyperspherical-harmonics wave functions. The work of J.C. is supported by the U.S. Department of Energy under contract W-7405-ENG-36, while that of R.S. is supported by the U.S. Department of Energy contract DE-AC05-84ER40150 under which the Southeastern Universities Research Association (SURA) operates the Thomas Jefferson National Accelerator Facility. The work of J.J. and I.S. is supported by the Schweizerische Nationalfonds. The calculations have been performed at the National Energy Research Supercomputer Center and at the facilities of the Accelerated Strategic Computing Initiative at Los Alamos National Lab.

## References

- [1] R.R. Whitney, I. Sick, J.R. Ficenec, R.D. Kephart, and W.P. Trower. *Phys. Rev. C*, 9:2230, 1974.
- [2] R. Altemus *et al.* *Phys. Rev. Lett.*, 44:965, 1980.
- [3] Z. Meziani *et al.* *Phys. Rev. Lett.*, 52:2130, 1984.
- [4] D. Onley, Y. Yin, and L.E. Wright. *Phys. Rev. C*, 45:1333, 1992.
- [5] K.S. Kim, L.E. Wright, Y. Yin, and D.W. Kosik. *Phys. Rev. C*, 54:2515, 1996.
- [6] M. Traini, S. Turck-Chièze, and A. Zghiche. *Phys. Rev. C*, 38:2799, 1988.
- [7] M. Traini and M. Covi. *Nuovo Cimento A*, 108:723, 1995.
- [8] J. Jourdan. *Nucl. Phys. A*, 603:117, 1996.
- [9] M. Traini. *nucl-th/0103045*.
- [10] J. Morgenstern and Z.E. Meziani. *nucl-ex/0105016*.
- [11] K.S. Kim, L.E. Wright, and D.A. Resler. *nucl-th/0103032*.
- [12] T. W. Donnelly and I. Sick. *Phys. Rev. C*, 60:065502, 1999.
- [13] T.W. Donnelly, J.W. Van Orden, T. de Forest, and W.C. Hermans. *Phys. Lett. B*, 76:393, 1978.
- [14] J.W. Van Orden and T.W. Donnelly. *Ann. Phys.*, 131:451, 1981.
- [15] M. Kohno and N. Ohtsuka. *Phys. Lett.*, 98B:335, 1981.
- [16] P.G. Blunden and M.N. Butler. *Phys. Lett. B*, 219:151, 1989.
- [17] W. Leidemann and G. Orlandini. *Nucl. Phys. A*, 506:447, 1990.
- [18] M.J. Dekker, P.J. Brussard, and J.A. Tjon. *Phys. Rev. C*, 49:2650, 1994.
- [19] J.E. Amaro and A.M. Lallena. *Nucl. Phys. A*, 537:585, 1992.
- [20] W.M. Alberico, M. Ericson, and A. Molinari. *Ann. Phys.*, 154:356, 1984.
- [21] J. Carlson and R. Schiavilla. *Phys. Rev. C*, 49:R2880, 1994.
- [22] V. Van der Sluys, J. Ryckebusch, and M. Waroquier. *Phys. Rev. C*, 51:2664, 1995.
- [23] M. Anguiano, A.M. Lallena, and G. Co. *Phys. Rev. C*, 53:3155, 1996.

- [24] A. Fabrocini. *Phys. Rev. C*, 55:338, 1997.
- [25] V. Gadiyak and V. Dmitriev. *Nucl. Phys. A*, 639:685, 1998.
- [26] E. Bauer. *Phys. Rev. C*, 61:044307, 2000.
- [27] J. Ryckebusch. *priv. com.*
- [28] C. Marchand *et al.* *Phys. Lett. B*, 153:29, 1985.
- [29] K.A. Dow *et al.* *Phys. Rev. Lett.*, 61:1706, 1988.
- [30] A. Zghiche *et al.* *Nucl. Phys. A*, 572:513, 1994.
- [31] K.F. vanReden *et al.* *Phys. Rev. C*, 41:1084, 1990.
- [32] D. Day *et al.* *Phys. Rev. Lett.*, 43:1143, 1979.
- [33] S. Rock *et al.* *Phys. Rev. C*, 26:1592, 1982.
- [34] D. Day *et al.* *Phys. Rev. C*, 48:1849, 1993.
- [35] R.M.Sealock *et al.* *Phys. Rev. Lett.*, 62:1350, 1989.
- [36] Z.-E. Meziani *et al.* *Phys. Rev. Lett.*, 69:41, 1992.
- [37] M.B. Barbaro, R. Cenni, A. DePace, T.W. Donnelly, and A. Molinari. *Nucl. Phys. A*, 643:137, 1998.
- [38] W.M. Alberico, A. Molinari, T.W. Donnelly, E.L. Kronenberg, and J.W. Van Orden. *Phys. Rev. C*, 38:1801, 1988.
- [39] R. Cenni, T.W. Donnelly, and A. Molinari. *Phys. Rev. C*, 56:276, 1997.
- [40] J. Carlson and R. Schiavilla. *Phys. Rev. Lett.*, 68:3682, 1992.
- [41] R. B. Wiringa, Steven C. Pieper, J. Carlson, and V. R. Pandharipande. *Phys. Rev. C*, 63:017603, 2000.
- [42] K. E. Schmidt and S. Fantoni. *Phys. Lett. B*, 446:99, 1999.
- [43] J. Golak *et al.* *Phys. Rev. C*, 52:1216, 1995.
- [44] S. Ishikawa *et al.* *Phys. Rev. C*, 57:39, 1998.
- [45] S. Martinelli, H. Kamada, G. Orlandini, and W. Glöckle. *Phys. Rev. C*, 52:1778, 1995.
- [46] V. D. Efros, W. Leidemann, and G. Orlandini. *Phys. Rev. Lett.*, 78:432, 1997.
- [47] M. Boninsegni and D. M. Ceperley. *J. Low Temp. Phys.*, 104:339, 1996.
- [48] M. Viviani, A. Kievsky, and S. Rosati. *Few-Body Syst.*, 18:25, 1995.
- [49] B. S. Pudliner, V. R. Pandharipande, J. Carlson, S. C. Pieper, and R. B. Wiringa. *Phys. Rev. C*, 56:1720, 1997.
- [50] M. Jarrell and J. E. Gubernatis. *Phys. Rep.*, 269:134, 1996.
- [51] J. Carlson and R. Schiavilla. *Rev. Mod. Phys.*, 70:743, 1998.
- [52] T. deForest and J.D. Walecka. *Adv. Phys.*, 15:1, 1006.
- [53] J.L. Friar. *Ann. Phys.*, 81:332, 1973.



- [54] M. Viviani, R. Schiavilla, and A. Kievsky. *Phys. Rev. C*, 54:534, 1996.
- [55] D.O. Riska. *Phys. Rep.*, 181:207, 1989.
- [56] R. Schiavilla, V.R. Pandharipande, and D.O. Riska. *Phys. Rev. C*, 40:2294, 1989.
- [57] H. Berg *et al.* *Nucl. Phys. A*, 334:21, 1980.
- [58] M. Chemtob and M. Rho. *Nucl. Phys. A*, 163:1, 1971.
- [59] M. Chemtob and M. Rho. *Nucl. Phys. A*, 212:628(E), 1973.
- [60] R. Schiavilla, R.B. Wiringa, V.R. Pandharipande, and J. Carlson. *Phys. Rev. C*, 45:2628, 1992.
- [61] L.E. Marcucci, D.O. Riska, and R. Schiavilla. *Phys. Rev. C*, 58:3069, 1998.
- [62] M. Viviani, A. Kievsky, L.E. Marcucci, S. Rosati, and R. Schiavilla. *Phys. Rev. C*, 61:064001, 2000.
- [63] L.E. Marcucci *et al.* *Phys. Rev. C*, 63:015801, 2001.
- [64] C.E. Carlson. *Phys. Rev. D*, 34:2704, 1986.
- [65] D. Abbott *et al.* *Phys. Rev. Lett.*, 82:1379, 1999.
- [66] R. Schiavilla. *priv. com.*
- [67] R. Schiavilla, V.R. Pandharipande, and D.O. Riska. *Phys. Rev. C*, 41:309, 1990.
- [68] G. Hoehler *et al.* *Nucl. Phys. B*, 114:505, 1976.
- [69] J. Jourdan. *Workshop on Electron-Nucleus Scattering*, eds. O. Benhar, A. Fabrocini, Edizioni ETS, Pisa, page 13, 1997.
- [70] R. Schiavilla, A. Fabrocini, and V.R. Pandharipande. *Nucl. Phys. A*, 473:290, 1987.
- [71] R. Schiavilla, V.R. Pandharipande, and A. Fabrocini. *Phys. Rev. C*, 40:1484, 1989.
- [72] R. Schiavilla, R.B. Wiringa, and J. Carlson. *Phys. Rev. Lett.*, 70:3856, 1993.
- [73] G. Orlandini and M. Traini. *Rep. Prog. Phys.*, 54:257, 1991.
- [74] R. Schiavilla. *Nucl. Phys. A*, 499:301, 1989.
- [75] J.L. Forest *et al.* *Phys. Rev. C*, 54:646, 1996.
- [76] A. Akmal and V.R. Pandharipande. *Phys. Rev. C*, 56:2261, 1998.
- [77] A. Fabrocini. *Phys. Rev. C*, 55:338, 1997.
- [78] A. Fabrocini. *priv. com.*